# NATIONAL ADVISORY COMMITTEE FOR AERONAUTICS

# WARTIME REPORT

ORIGINALLY ISSUED

July 1945 as Memorandum Report L5F20

WIND-TUNNEL TESTS OF THE 0.15-SCALE POWERED MODEL

OF THE FLEETWINGS XBTK-1 ATRPLANE

LATERAL STABILITY AND CONTROL

By Kenneth W. Goodson and H. Norman Silvers

Langley Memorial Aeronautical Laboratory
Langley Field, Va.





#### WASHINGTON

NACA WARTIME REPORTS are reprints of papers originally issued to provide rapid distribution of advance research results to an authorized group requiring them for the war effort. They were previously held under a security status but are now unclassified. Some of these reports were not technically edited. All have been reproduced without change in order to expedite general distribution.

MR No. L5F20

NATIONAL ADVISORY COMMITTEE FOR AERONAUTICS

### MEMORANDUM REPORT

for the

Bureau of Aeronautics, Navy Department
WIND-TUNNEL TESTS OF THE 0.15-SCALE POWERED MODEL
OF THE FLEETWINGS XBTK-1 AIRPLANE
LATERAL STABILITY AND CONTROL

By Kenneth W. Goodson and H. Norman Silvers

#### SUMMARY

Tests were conducted in the Langley 7- by 10-foot tunnel on the 0.15-scale powered model of the Fleetwings XBTK-1 airplane to investigate the lateral stability characteristics.

The results of this investigation indicated that the effective dihedral, with a geometric dihedral of  $8\frac{1}{4}^{\circ}$ , was positive for all conditions except wave-off. In this condition, the model had negative effective dihedral at lift coefficients above 2.10. The negative values of effective dihedral were not decreased when the geometric dihedral was changed to  $11^{\circ}$ .

The directional stability was satisfactory for all conditions. Increasing the geometric dihedral generally decreased the directional stability.

The tests indicated that the airplane will probably not experience rudder lock.

Results of the rudder modification tests indicate that the positive variation of rudder hinge-moment coefficient with yaw, which may result in snaking of the airplane, may be reduced by either unsealing the rounded horn or removing the horn and sealing the gap.

The rudder effectiveness will probably be sufficient to trim the airplane with the wings level in any condition. In the wave-off condition, the rudder-tab deflection would be insufficient to trim the pedal force to zero at zero bank.

The aileron effectiveness will probably be satisfactory throughout the angle-of-attack range.

#### INTRODUCTION

At the request of the Bureau of Aeronautics, Navy Department, a series of tests was made in the Langley 7- by 10-foot tunnel of a 0.15-scale powered model of the Fleetwings XBTK-l airplane. The investigation was conducted to provide data on the stability and control characteristics of the model. The longitudinal stability and control results of this investigation are presented in reference 1. The present report includes the results of tests made to determine the lateral stability and control characteristics of the model. From the results of these tests the probable flying qualities of the airplane may be estimated.

#### COEFFICIENTS AND SYMBOLS

The results of the tests are presented as standard NACA coefficients of forces and moments. Rolling, yawing, and pitching-moment coefficients are given about the center-of-gravity location shown in figure 1 (25.6 percent of the mean aerodynamic chord). The data are referred to a system of axes in which the Z-axis is in the plane of symmetry and perpendicular to the relative wind, the X-axis is in the plane of symmetry and perpendicular to the pendicular to the Z-axis, and the Y-axis is perpendicular to the plane of symmetry.

The coefficients and symbols are defined as follows:

CT lift coefficient (Z/qS)

CDp resultant-drag coefficient (X/qS)

```
lateral-force coefficient (Y/qS)
Cy
       rolling-moment coefficient (L/qSbw)
C 7.
       pitching-moment coefficient (M/qSc)
Cm
       yawing-moment coefficient (N/qSbw)
Cn
       hinge-moment coefficient (H/qbc2)
Ch
Tc
       effective thrust coefficient (Te/qS)
nD/V
       propeller diameter-advance ratio
       propulsive efficiency (TeV/2mnQ)
7
       torque coefficient (Q/pV2D3)
Qc.
where the quantities are defined below and in figure 2
(X
Y>
       forces along axes, pounds
Z
L
M
       moments about axes, pound-feet
N
       hinge moment of a control surface, pound-feet
H
Q.
       torque, pound-feet
Te
       effective thrust, pounds
       dynamic pressure (pv2/2), pounds per square feet
q
       wing area (8.55 sq ft on model)
S
       wing mean aerodynamic chord (1.22 ft on model)
       root mean square chord of a control surface back
C
          of hinge line, feet
       wing span (7.33 ft on model)
bw
b
       span of control surface, feet
V
       air velocity, feet per second
```

```
4
                                             MR No. L5F20
       propeller diameter (2.04 ft on model)
D
       revolutions per second
n
       weight of the airplane, pounds
W
and
       mass density of air, slugs per cubic foot
       angle of attack of thrust line, degrees
α
       wing setting with respect to thrust line (20 on
1 w
          model)
V
       angle of yaw, degrees
       control surface deflection, degrees
8
       propeller blade angle at 0.75 radius (180)
B
       effective dihedral, degrees
Ta
To
       geometric dihedral, degrees
Subscripts:
```

a aileron (ar, a, right and left aileron)

w wing

r rudder

f flap

t tab

denotes partial derivative of a coefficient with respect to yaw (example:  $C_{l_{\psi}} = \frac{\partial C_{l}}{\partial \psi}$ )

#### MODEL AND APPARATUS

The XBTK-l airplane is a single-place single-engine, carrier-based, dive and torpedo bomber with a full cantilever low wing. It has partial-span, extensible slotted flaps, "picket-fence" dive brakes, adjustable

stabilizer, and a fully retractable conventional landing gear. At the design gross weight, the airplane carries a radar unit under the right wing panel and an auxiliary droppable fuel tank under the left wing panel in addition to one 1000-pound bomb under the fuselage. The rudder is aerodynamically balanced by a combination of an overhang balance, a horn, and a tab. The balance tab has a deflection rate of 0.51 of the rudder deflection and may also be hand-cranked to a maximum deflection of ±5° for trimming. Each aileron is aerodynamically balanced by an internal sealed balance and a spring tab. The balance area is 41 percent of the aileron area. A summary of the physical characteristics of the airplane is presented in tables I, II, and III.

The model was furnished by the Fleetwings Division of the Kaiser Cargo Corporation. A three-view drawing of the 0.15-scale model is shown in figure 1 and photographs of the model are given in figures 3(a), 3(b), and 3(c). Small wooden dowels were placed in the leading edge of the wing (18.09 in. from the center line) to simulate cannon on the airplane.

The model was equipped with a slotted extensible type of landing flap which extends across the fuselage (figs. 3 and 4(a)) with a 22.5-percent chord and a 43.1-percent span. The center and the outer flaps can be operated separately. Special fittings were supplied for changing the geometric dihedral.

The dive brakes (figs. 3(c) and 4(b)), which are of the picket-fence type, are mounted on the upper and lower surfaces of the center wing panel near the trailing edge. The hinge line of the upper surface brake is located at the trailing edge. The hinge line of the lower dive brake is, however, located at the leading edge of the lower brake in the conventional manner. The dive brakes on the airplane are linked together in such a manner as to reduce the total hinge moment of the system.

The vertical tail has a modified NACA 66,2-015 root section and a modified NACA 65,2-009 theoretical tip section. The modification confisted of replacing the cusp trailing edge with a straight line fairing tangent to the airfoil contour at the 0.70-chord section. The rudder had an area of 30.5 percent of the vertical tail and was mass-balanced. The model was tested with several

modifications of the vertical tail as shown in figure 5. The rudder was first modified by rounding the lower surface of the horn balance. It was further modified by making hinge cut-outs in the balance and in the seal (modification 3). The rudder was sealed up to the horn. The data presented herein are based upon the above modifications (fig. 6) since these modifications represent the prototype airplane. A further modification was made by removing the horn.

The aileron on the model, which was located outboard of the center wing panel, had a span 54 percent of the wing semispan. The aileron was of constant percentage chord  $\left(\frac{ca}{c_w} = 0.20\right)$ . All tests reported herein were made with an aileron seal of cellulose tape. No provisions were made on this model for the measurement of aileron hinge moments.

The model was equipped with a 2.04-foot-diameter propeller with blades set at 18° and was powered by a 56-horsepower induction motor. The propeller speeds were determined by a small alternator tachometer and a cathode-ray oscillograph combination.

The model configurations referred to in the text and on the figures are as follows:

- 1. Cruising configuration
  Flaps neutral
  Landing gear retracted
  Fuel tank on left wing
  Radar on right wing
- 2. Landing configuration
  Flaps deflected (45°)
  Landing gear extended
  (a) Main wheels down
  - (b) Wheel-well cut-outs in wing open
  - (c) Tail wheel down
  - (d) Tail-wheel door open (e) Arresting hook extended

Fuel tank on left wing Radar on right wing

J. Diving configuration

Upper dive flaps deflected (73°)

Lower dive flaps deflected (80°)

Center flap deflected (45°)

Landing gear retracted

Radar on right wing

The rudder, rudder-tab, and aileron deflections were set by means of templets to ±0° 30°. Flap and dihedral fittings were supplied by the manufacturer. Strain gages and strain-gage fittings were constructed and installed by the Langley Laboratory.

#### TESTS AND RESULTS

Test conditions. The tests were made at dynamic pressures of 9.21 and 16.37 pounds per square foot, corresponding to airspeeds of about 60 and 80 miles per hour. The test Reynolds numbers were about 685,000 and 910,000 based on the wing mean aerodynamic chord of 1.22 feet. Because of the turbulence factor of 1.6 for the tunnel, effective Reynolds numbers (for maximum lift coefficient) were about 1,100,000 and 1,460,000.

Test procedure. The model propeller was calibrated by measuring the resultant drag of the model in the cruising condition at zero angle of attack for a range of propeller speeds. The thrust coefficients were determined from the relation

$$T_c' = C_D - C_{D_R}$$

where  $C_D$  is the drag of the model with the propeller removed. The torque coefficient  $Q_c$  was computed from the motor calibration chart (torque as a function of minimum current) using the minimum current of the motor for each propeller speed. The propeller calibration is presented as a function of nD/V (fig. 7). The variation of lift coefficient with thrust coefficient for the airplane is presented in figure 8(a). With the aid of these two figures, a propeller speed required to simulate the specified power condition may be determined for a particular tunnel speed. All tests reported herein were made at thrust coefficients simulating take-off power on the prototype airplane. The torque coefficient

of the model, as a function of lift coefficient, was in good agreement with the torque coefficient of the airplane (fig. 8(b)). All tests simulating windmilling power were made at a thrust coefficient of -0.010.

Corrections. - All data have been corrected for tares caused by the model support strut. Jet-boundary corrections have been applied to the angles of attack, the drag coefficient, and the tail-on pitching-moment coefficients.

Presentation of data. The results of the lateral stability investigation made on the 0.15-scale model of the XBTK-l airplane are presented in the following figures:

		Figure no.
Α.	Rudder-fixed stability:  1. Lateral stability parameters	
В.	Rudder-free stability	11
C.	Control characteristics:  1. Effect of rudder modification on the aerodynamic characteristics in yaw  2. Effect of rudder deflection on the aerodynamic characteristics in  (a) Yaw	12
	(b) Pitch	ero-
D.	Aileron characteristics in pitch 17	and 18

#### DISCUSSION

# Rudder-Fixed Stability

Effective dihedral. The effective dihedral with the original geometric dihedral angle of  $8\frac{10}{4}$  was positive for all conditions except for the take-off power, landing configuration where it becomes negative above a lift

coefficient of about 2.1. The effective dihedral for the high-speed condition was fairly high (8.7°). This value was obtained from figure 9 by using the theoretical value for OCI/OW of 0.00023 per degree of effective dihedral (reference 2). A comparison of tail-off and tail-on data shows that the vertical tail has a large positive effect on the effective dihedral for all configurations and powers. Because of the large incremental change in rolling moment with rudder deflection (fig. 13), the slope of the rolling-moment curve will become less positive or more negative when the model is trimmed in yaw; therefore, the effective dihedral will be decreased. The effective dihedral for the trimmed wave-off condition (take-off power, landing configuration) is about -3.50 to -4.00 at a lift coefficient of about 2.06 (fig. 13(e)); however, figure 9(d) indicates that the effective dihedral will probably be decreased at higher lift coefficients. In an effort to increase the effective dihedral in the wave-off condition, it was decided to increase the geometric dihedral angle to 110. Calculations by the method of reference 2 indicated that  $C_{l\psi}$  should be increased by 0.00048 when the geometric dihedral of the outer panels was changed from  $8\frac{1}{4}^{\circ}$  to 11°. The measured positive increase in Cly corresponded very closely to the calculated value in all conditions except for the wave-off condition at lift coefficients above 2.28 for which case the effective dihedral was actually reduced (fig. 9(d)). The explanation for this negative increase in effective dihedral is not known at present; however, similar results have been observed on another model tested in the Langley 7- by 10-foot tunnel. Good agreement in Cl was obtained between the data from yaw-range tests (fig. 13) and those from pitch tests made at  $\psi = \pm 5^{\circ}$ (fig. 9).

Directional stability.— The test data indicated that the model was very stable directionally for all conditions; the value of  $c_{n\psi}$  was always greater than -0.0015. Lowering the flaps (fig. 9(c) and 9(d)) generally increased the directional stability throughout the lift range. The directional stability did, however, decrease somewhat as the lift increased in the landing condition. The directional stability increases in all conditions when power is applied (fig. 9). This increase is most pronounced in the wave-off condition (take-off power, landing configuration). The

parameter  $C_{n_\psi}$  determined from tests made through the yaw range agree well with the  $C_{n_\psi}$  of lateral stability parameter tests. The directional stability parameter obtained from yaw tests is tabulated below for the sake of comparison for various model configurations and power conditions.

Figure	Model	α	C <sub>I.</sub> Power		$\frac{\partial c_n}{\partial \psi}$ $\delta_r = 0$		
no.	configuration				Tail-on	Tail-off	
13(a)	Cruising	11.0	1.14	Windmilling	-0.00187	0.00080	
13 (b)	Cruising	5	.23	Take-off	00208	.00068	
13(c)	Cruising	7.7	1.03	Take-off	00280	.00112	
13(d)	Landing	10.5	1.63	Windmilling	00220	.00080	
13(e)	Landing	10.0	2.06	Take-off	00590	.00049	
1/4	Dive	1.0	•15	Windmilling	00212		

Increasing the geometric dihedral angle to  $11^{\circ}$ , in general, decreased the directional stability. For the wave-off conditions,  $C_{n_{\psi}}$  was increased slightly at lift coefficients above 2.22 when the geometric dihedral was increased.

Lateral force. The positive values of  $c_{Y\psi}$  for all conditions indicate that the airplane will have right sideslip with right bank and vice versa. The tail increases the positive value of  $c_{Y\psi}$  as shown by comparing tail-on and tail-off data.

Pitching moment due to yaw. The data of figure 13 indicate substantial changes in pitching moment with yaw for the power-on conditions. However, estimations indicate that less than 1° change in elevator deflection would be sufficient to trim the pitching moments resulting from a change in rudder deflection of ±5°

# Rudder-Free Stability

Rudder-free characteristics .- The rudder-free characteristics for the most critical conditions were obtained from data of figures 13 and 16. These rudder-free data were obtained by taking into consideration the balancetab deflection and a trim-tab deflection of 50. Curves are presented also considering only a trim-tab deflection of 50. From preliminary calculations, trim-tab deflections of 50 and 150 were required for the take-off power cruising configuration and the take-off power landing configuration, respectively; however, since only 150 of trim-tab deflection was provided for on the prototype airplane, the rudder-free curves were determined for this value. The results (fig. 11) indicate that the airplane will probably not have rudder lock; however, there is a tendency for rudder lock at both negative and positive yaw values of about 10° to 15°. A comparison of the results obtained with the balance tab locked and operating indicates that the rudder-lock tendency is aggravated by balance-tab deflection. The rudder-free characteristics with the balance tab locked are comparable to those of a spring tab. It is thought that by using a spring tab to obtain aerodynamic balance of the rudder the trend toward rudder lock may be reduced.

#### CONTROL CHARACTERISTICS

Rudder modifications. The original rudder horn had a flat under surface. It was thought that this might lead to early compressibility effects. Also, it was noted from preliminary tests that with the original rudder  $\text{Ch}_{\psi}$  was positive. Since snaking of the airplane may result from this aerodynamic characteristics of the rudder, it was desired to determine the effect of various modifications (fig. 4(a)) in reducing the positive value of  $\text{Ch}_{\psi}$ . Results of rudder tests conducted through the yaw range (fig. 12) indicate that  $\text{Ch}_{\psi}$  may be appreciably reduced by either unsealing the rounded horn or removing the horn and sealing the rudder gap. The latter modification reduces  $\text{Ch}_{\psi}$  to approximately zero. The effectiveness of the rudder was increased by rounding the under surface of the horn (modification 1). The other modifications decreased the effectiveness.

A comparison of the results of the rudder modifications at small rudder deflections is presented in the following table.

Rudder modification	∂c <sub>n</sub> /∂δ <sub>r</sub>	$\partial C_{\rm h}/\partial \psi$	∂C <sub>h</sub> /∂δ <sub>r</sub>
Original	-0.00156	0.0031	-0.0024
1	00185	.0027	0024
2	00105	.0018	0016
3	00163	.0027	0030
1	00142	.0009	0025
5	00138	0	0035

The increment of  $C_{h\psi}$  obtained when the horn was removed (approximately -0.0027) (figs. 12(d) and 12(f)) checked closely with the estimated value (-0.0021) using data of reference 3.

The rudder modifications have very little effect on the cross-wind and rolling-moment coefficients.

Rudder and rudder-tab characteristics. The rudder (modification 3) and rudder-tab effectiveness as determined from figures 13, 14, and 16 are presented in the following table:

Model configuration	α	CL	Power	$\partial G_{n}/\partial \delta_{r}$ $\psi = 0$	$\begin{array}{c} \partial c_{hr} / \partial \delta_{t} \\ \psi = 0 \end{array}$
Cruising	11.0	1.14	Windmilling	-0.00153	-0.00265
Cruising	5	.23	Take-off	00163	00340
Cruising	7.7	1.03	Take-off	00231	00600
Landing	10.5	1.63	Windmilling	00155	00334
Landing	10.0	2.06	Take-off	00311	00950
Dive	1.0	.15	Windmilling	00142	

MR No. L5F20

The rudder and rudder-tab effectiveness are greatly increased with take-off power in the landing configuration.

Preliminary calculations indicate that there will probably be sufficient rudder effectiveness to trim the airplane in yaw with the wings level for any condition. Further estimations indicate that there is sufficient trim-tab deflection to trim the pedal force to zero with the wings level except for the wave-off condition.

The rudder hinge-moment coefficient does not show an appreciable change in the dive configuration as compared with that of the cruising configuration.

A positive rudder-tab deflection of 10° (fig. 15) has a small constant effect (-0.003) on the yawing moment throughout the lift range for the take-off power, cruising configuration. The rudder hinge moment resulting from a 10° tab deflection (zero rudder) will overbalance the hinge moment caused by 10° of rudder deflection (zero tab). The lateral force is reasonably constant throughout the pitch range.

Aileron characteristics.— The aileron characteristics were obtained from tail-off tests for two model configurations (cruising and landing). The results of these tests (figs. 17 and 18) indicate that the effectiveness of the control surface is very good throughout the angle-of-attack range. Flap deflection has no appreciable effect upon this condition. Preliminary calculations from unpublished data indicate that the required helix angle of 0.08 may be obtained by the airplane in either the landing or high-speed conditions.

The adverse yaw resulting from aileron deflection is increased when the flap is deflected.

#### CONCLUSIONS

The results of wind-tunnel tests to determine the lateral stability and control characteristics of the XBTK-1 airplane indicate that the following conclusions may be drawn:

- l. The effective dihedral was positive for all conditions except wave-off where it was negative at lift coefficients above 2.10. The negative effective dihedral for this condition was greater when the geometric dihedral angle of the outer panel was changed from  $8\frac{10}{11}$  to  $11^{\circ}$ .
- 2. The directional stability should be satisfactory for all flight conditions. Increasing the geometric dihedral angle generally decreased the directional stability.
- 3. The positive values of  $c_{Y\psi}$  for all conditions indicate that the airplane will have right sideslip with right bank, and vice versa.
- 4. The estimated rudder-free characteristics indicate that there will probably be no rudder lock although snaking of the airplane may result from the positive variation of rudder hinge moment with angle of yaw with the horn balance in place.
- 5. The variation of rudder hinge moment with angle of yaw was reduced to approximately zero when the horn was removed. The rudder effectiveness was increased when the horn was rounded but was decreased when the gap was unsealed, when hinge cut-outs were made in the seal and balance, and when the horn was removed.
- 6. Estimations indicate that there is probably sufficient rudder effectiveness to trim the airplane with wings level and, except for the wave-off condition, there is sufficient tab deflection to trim the pedal force to zero with wings level.
- 7. The effectiveness of the aileron should be satisfactory through the angle-of-attack range. The adverse yaw resulting from aileron deflection is increased when the flap is deflected.

Langley Memorial Aeronautical Laboratory
National Advisory Committee for Aeronautics
Langley Field, Va.

#### REFERENCES

- 1. Weil, Joseph, and Boykin, Rebecca I.: Wind-Tunnel Tests of the 0.15-Scale Powered Model of the Fleetwings XBTK-1 Airplane. Longitudinal Stability and Control. NACA MR No. L5D27a, 1945.
- 2. Pearson, Henry A., and Jones, Robert T.: Theoretical Stability and Control Characteristics of Wings with Various Amounts of Taper and Twist. NACA Rep. No. 635, 1938.
- 3. Lowry, John G., Maloney, James A., and Garner, I. Elizabeth: Wind-Tunnel Investigation of Shielded Horn Balances and Tabs on a O.7-Scale Model of XF6F Vertical Tail Surface. NACA ACR No. 4Cll, 1944.

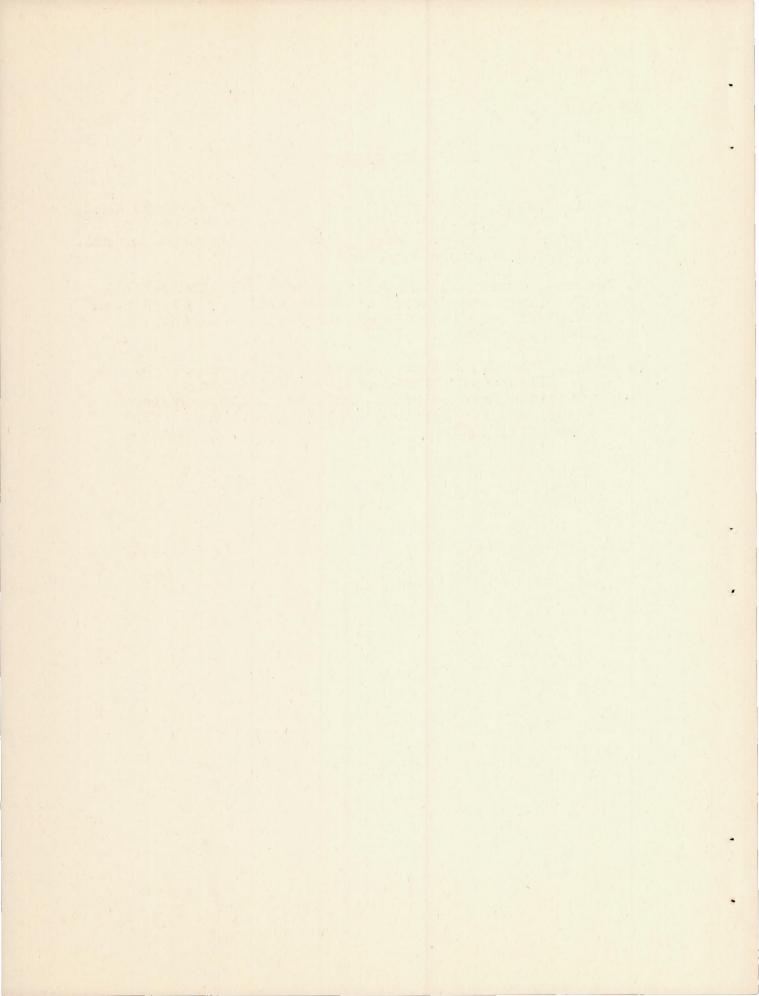


## TABLE I

# DESCRIPTION OF FLEETWINGS XBTK-1 AIRPLANE

Name and type	XBTK-1 (Navy dive-torpedo bomber)
Engine	Pratt & Whitney R-2800-22W
Normal power Take-off power	{1700 bhp at 2600 rpm at sea level 1700 bhp at 2600 rpm at 7000 ft 1450 bhp at 2600 rpm at 18,500 ft 2100 bhp at 2800 rpm at sea level { 2100 bhp at 2800 rpm at 1000 ft 1600 bhp at 2800 rpm at 16,000 ft
Diameter, ft Blades (number and Gear ratio	Hamilton Standard 13.58 designation)
Normal gross weight, 1	b 14,850
Over-all length, ft .	
Over-all height, ft.	
Wing span, ft	

NATIONAL ADVISORY COMMITTEE FOR AERONAUTICS

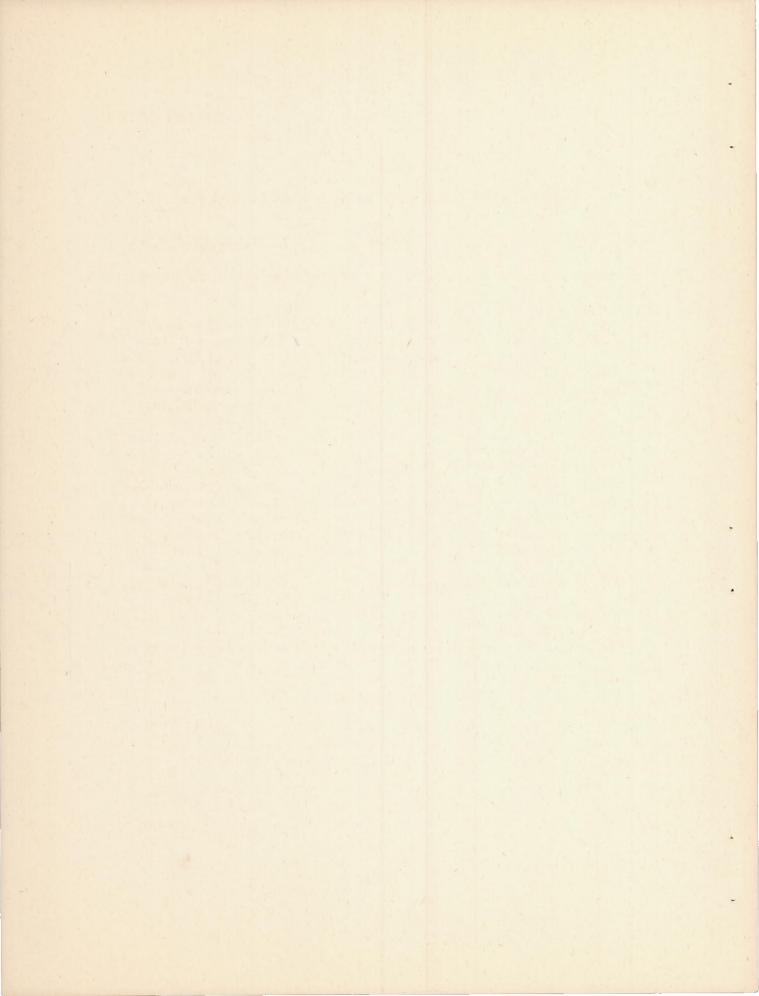


TABLE II

AIRPLANE WING AND TAIL-SURFACE DATA

	Wing	Horizontal tail	Vertical tail
Area, sq ft	380	80	a <sub>51.25</sub>
Span, ft	48.67	18.5	8.54
Aspect ratio	6.23	4.26	1.42
Taper ratio	.50	•59	
Dihedral, deg	8.25	0	
Incidence, deg	2	2 to -7	0
Geometric twist, deg	-2.2	0	0
Root section	NACA 2416	NACA 66,2-015 Modified	NACA 66,2-015 Modified
Tip section	NACA 4412	NACA 66,2-009 Modified	NACA 65,2-009 Modified
Mean aerodynamic chord, ft 8.17			
Root chord, ft	9.17	5.45	6.89
Theoretical tip	4.585	3.20	2.67

a Includes dorsal fin.

NATIONAL ADVISORY COMMITTEE FOR AERONAUTICS

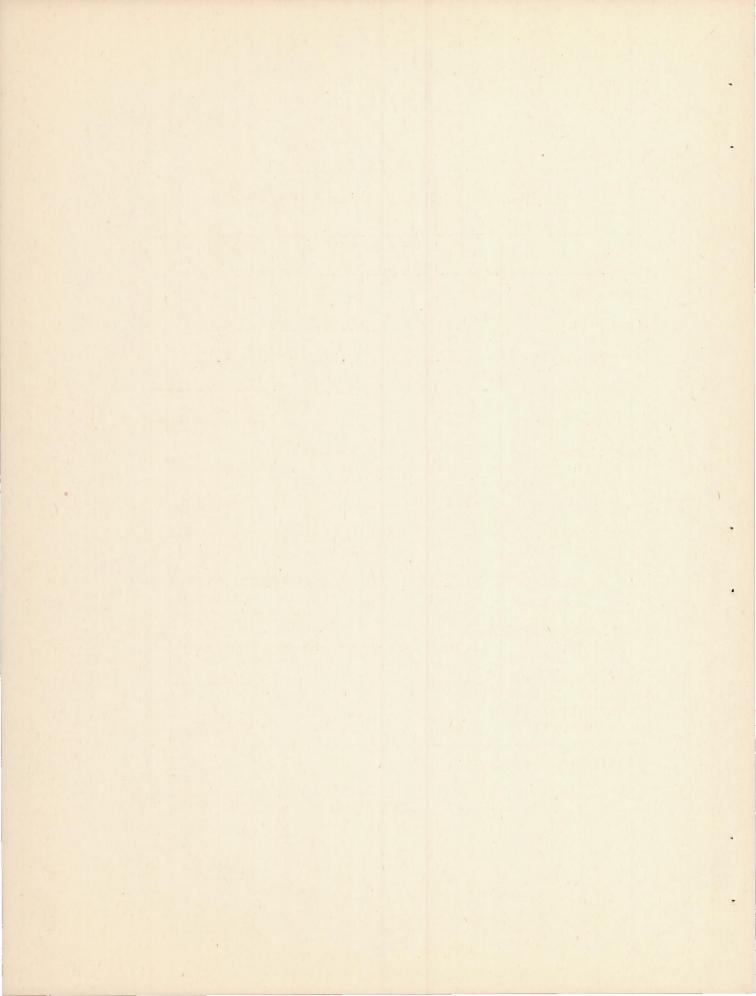


TABLE III AIRPLANE CONTROL-SURFACE DATA

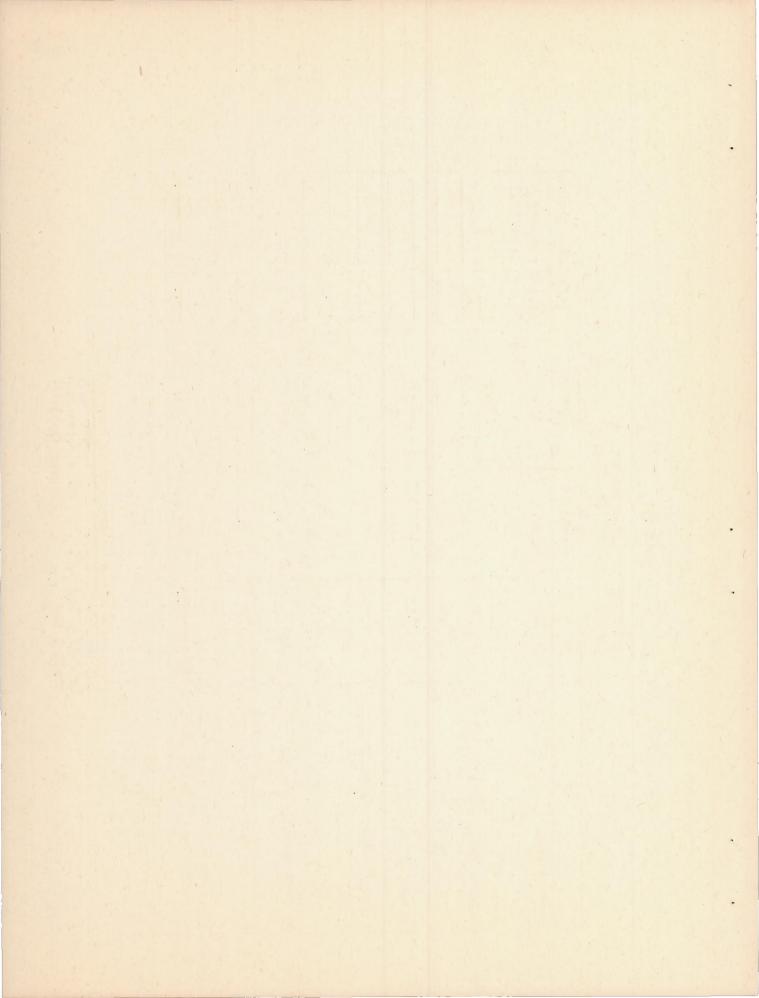
	Ailerons	Elevators	Rudder	Flaps	Dive brakes
Percent span	54.0	95.0	100	43.1	Upper 31.4 Lower 35.1
Area, aft of hinge line, sq ft	36.86	22.50	15.66	42.0	
Balance area, sq ft	15.11	2.96	a5.02		
Trim-tab area, sq ft	b.52	None	1.00		
Percent span	2.8		23.0		
Tab travel, deg	±15		±5		
Balance tab area, sq ft	2.76	3.36	1.00		
Percent span	13 • 3	35.7	23.0		and the real the real the tark too too test too
Tab travel, deg	±15(±30 lb)	±15(±55 1b)	$\pm 15(\delta_{t} = -0.51\delta_{r})$		dark was still table over over over our upp start tiggs
Control travel, deg	<b>±</b> 15	15, -25	±30	45	cupper 73 Lower 80
Root mean square chord, ft	1.37	1.27	1.90	2.06	Upper 1.45 Lower 1.55
Distance to hinge line from normal e.g. (25.6), ft		22.00	23.67		alls (15 m) and our old our ow our load hap

al.20 sq ft horn.

Flap deflections (corresponding powers)
Landing, deg . . . . . 45 (power off) Cruising, deg . . . flaps retracted Diving, deg . . (center flap) 45

bLeft aileron only.

CMeasured from aileron contour.



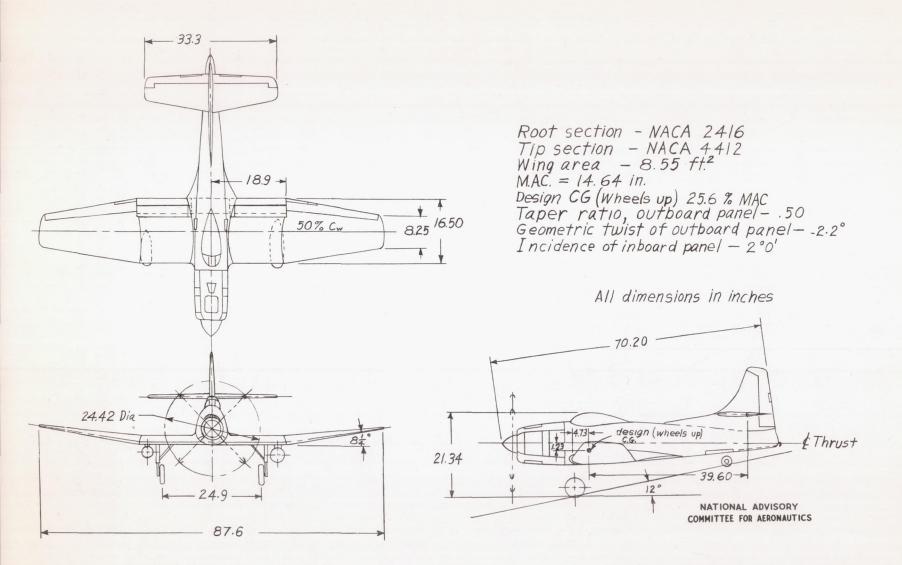


Figure 1 .- Three view drawing of 0.15 - scale model of Fleetwings XBTK-1 airplane.

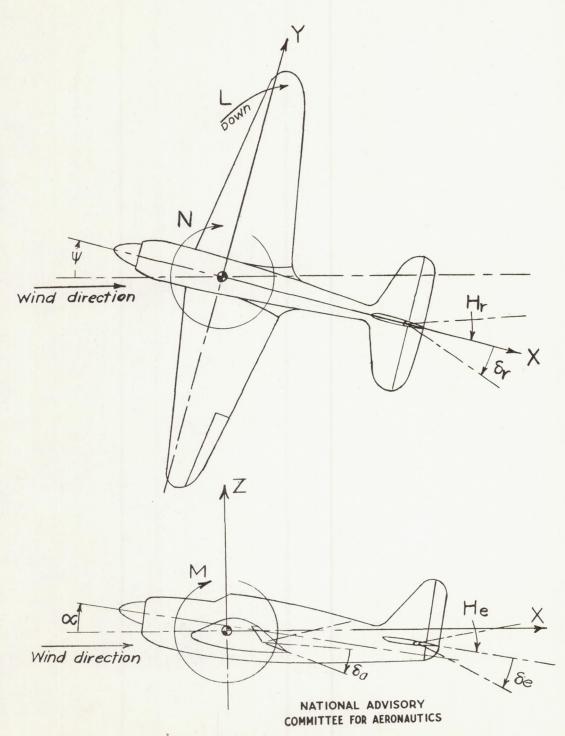


Figure 2.- Notation of the system of axes and the control-surface hinge moments and deflections. (Arrows indicate positive values.)

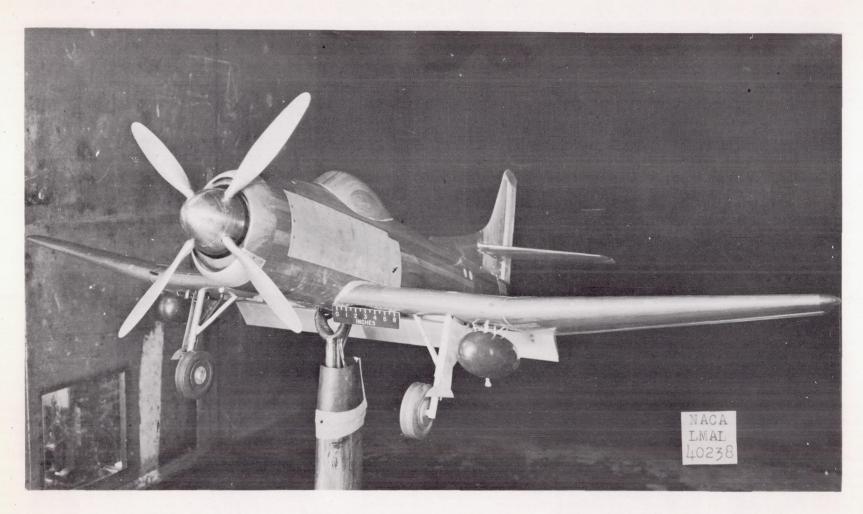


Figure 3(a).- Three-quarter front view of a 0.15-scale model of the XBTK-1 airplane.

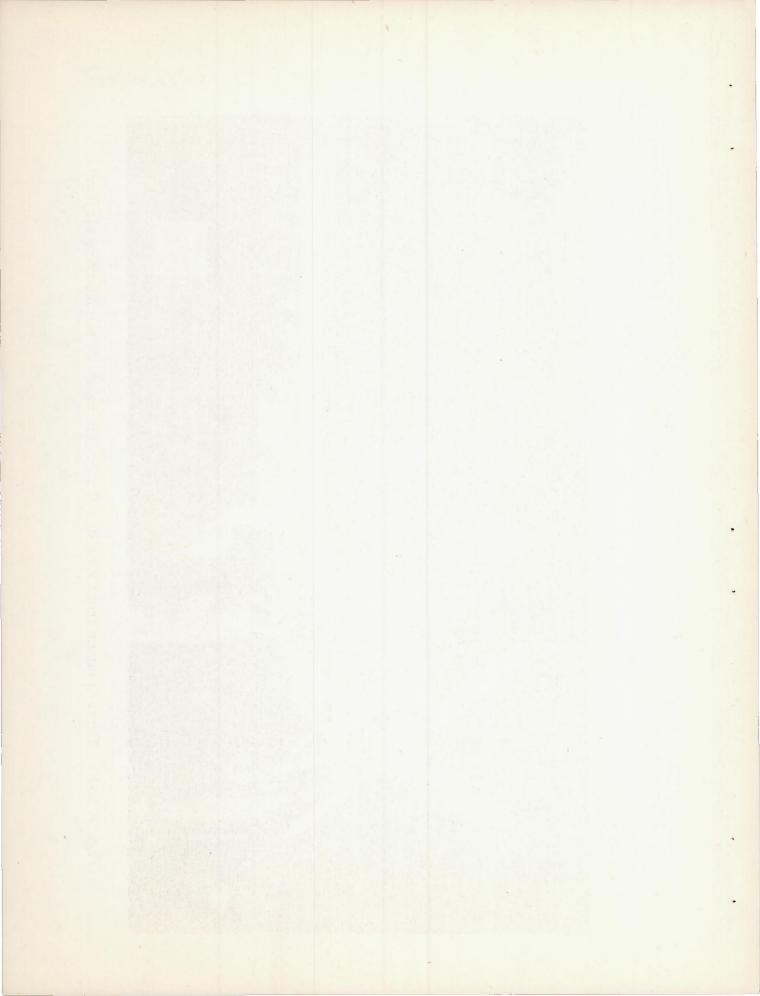
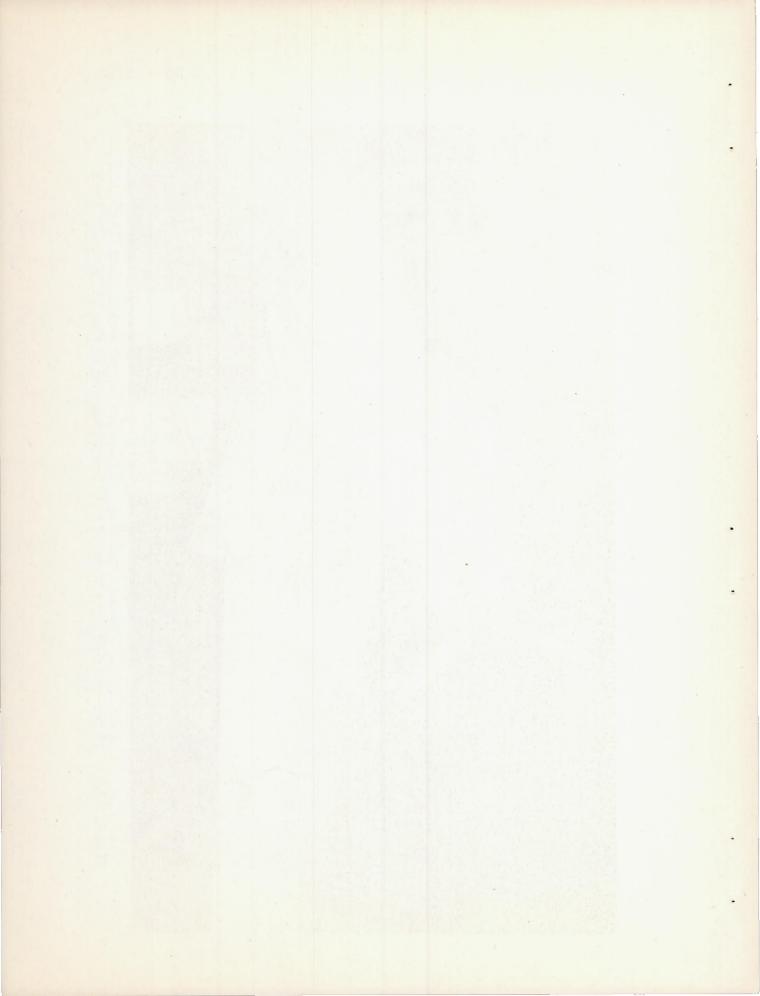




Figure 3(b).- Three-quarter rear view of a 0.15-scale model of the XBTK-1 airplane.



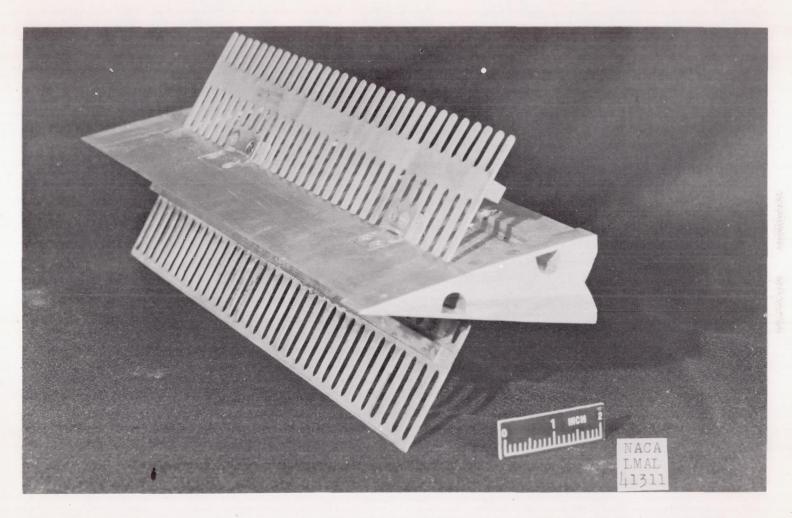
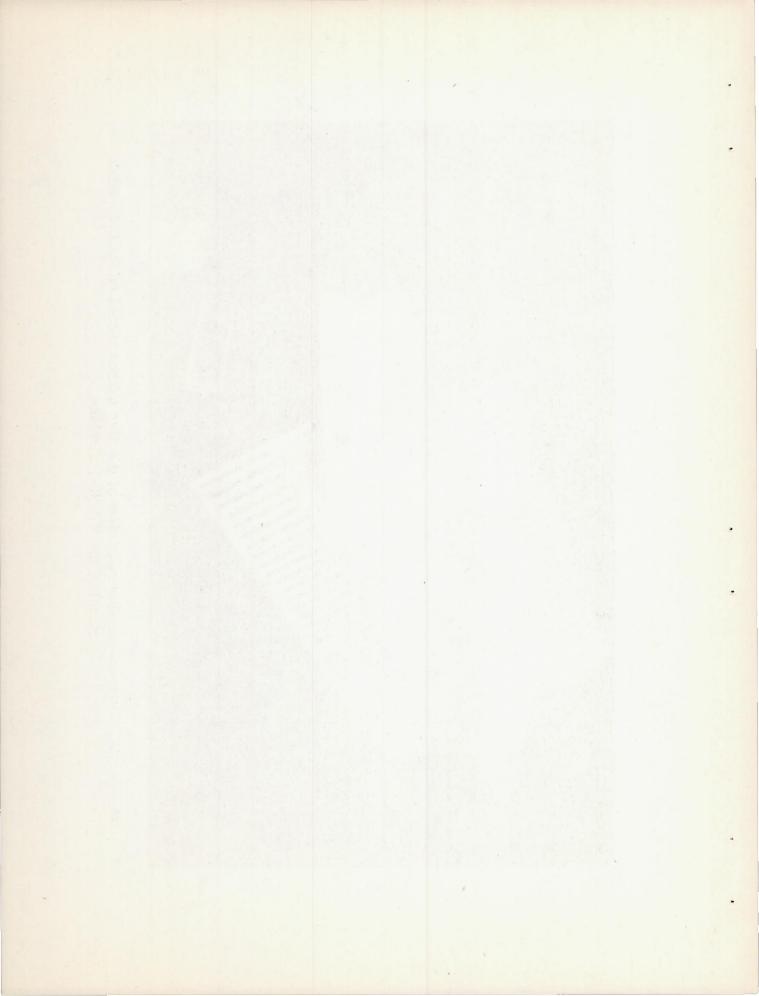


Figure 3(c).- Three-quarter rear view of the dive brakes tested on the 0.15-scale model of the XBTK-1 airplane.



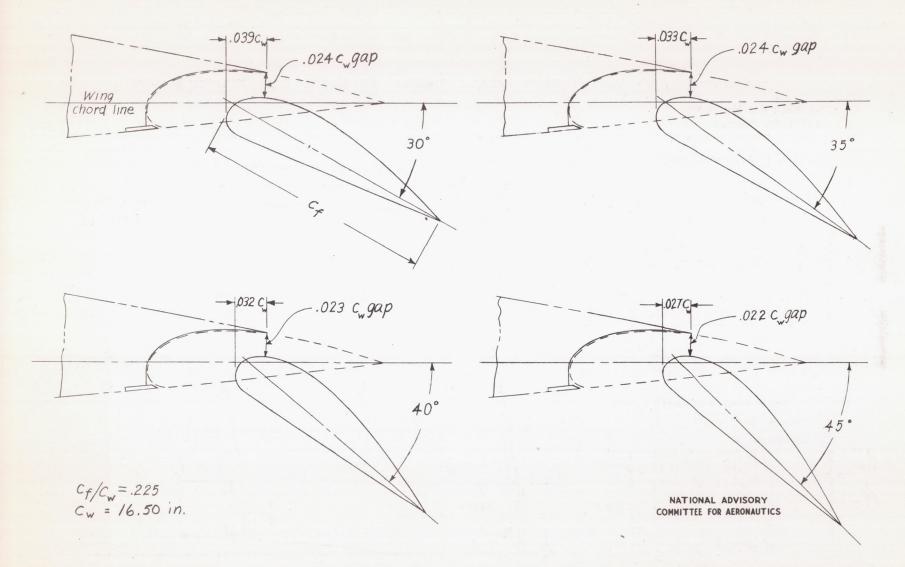


Figure 4(a), Details of slotted flap positions for various deflections tested on the 0.15 scale model of the XBTK-1 airplane.

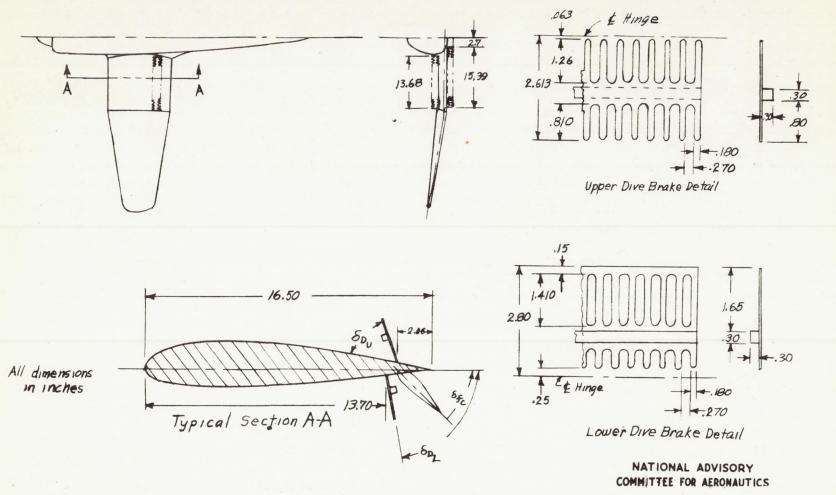
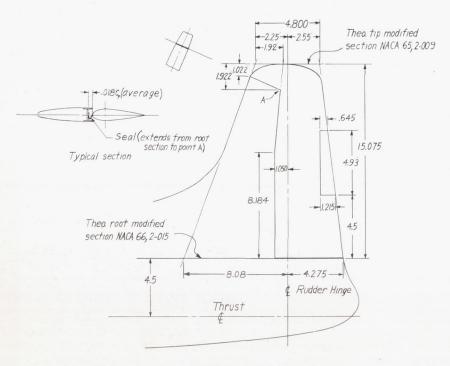


Figure 46) Detail of dive brakes on the 0.15 scale model of the XBTK-I airplane.

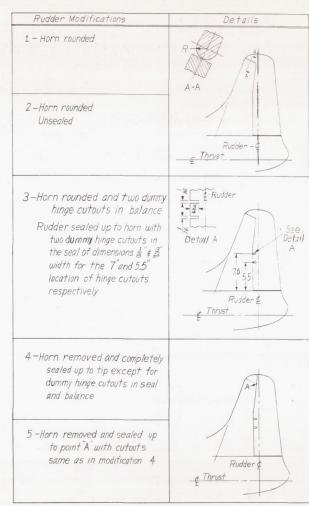
Total vertical tail area - - - - - - 1.15 sq.ft.\*
Rudder area aft of hinge - - - - .352 sq.ft
Root mean square chord aft of hinge - - 3.42 in.
Unshielded area of rudder horn - - - - .016 sq.ft.
Shielded area of rudder horn - - - - 011 sq.ft

\* includes dorsal fin

Not to scale



Original vertical tail



NATIONAL ADVISORY
COMMITTEE FOR AERONAUTICS

Figure 5.\_ Comparison of rudder modifications as tested on the 0.15 scale model of the XBTK-1 airplane.

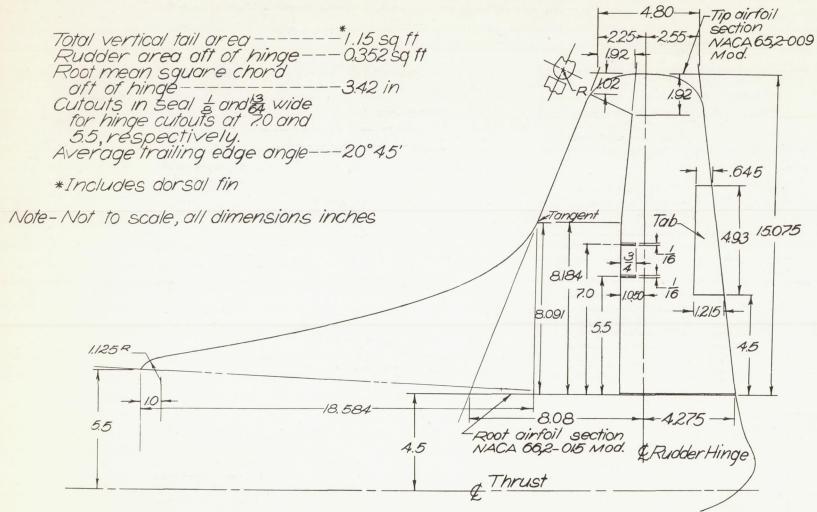
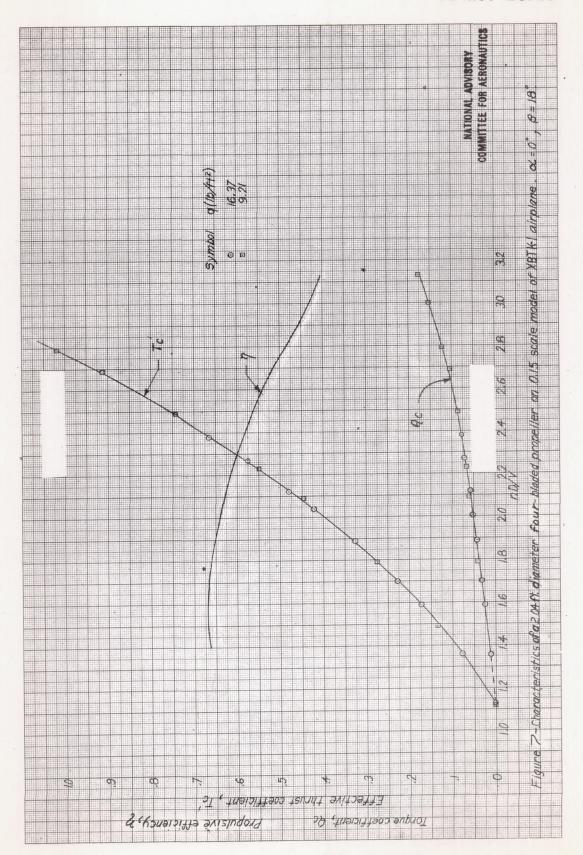
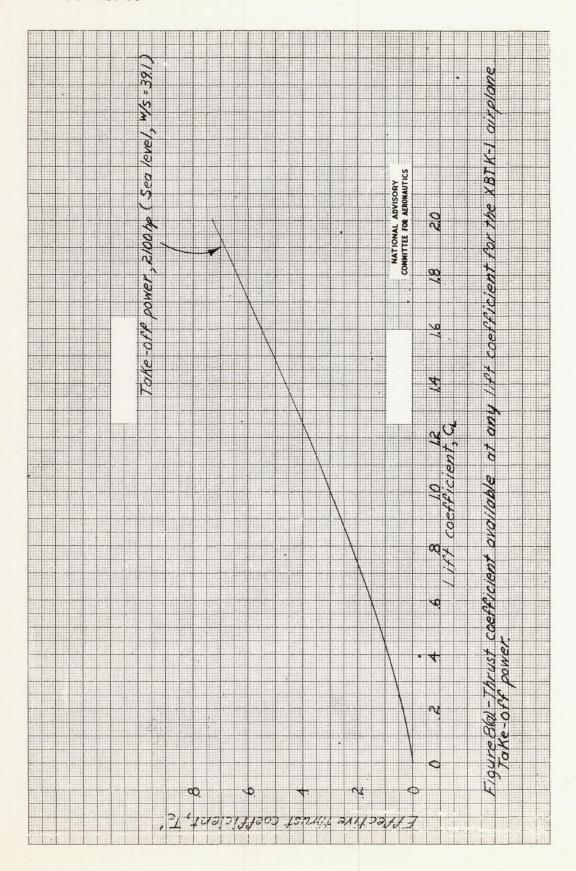
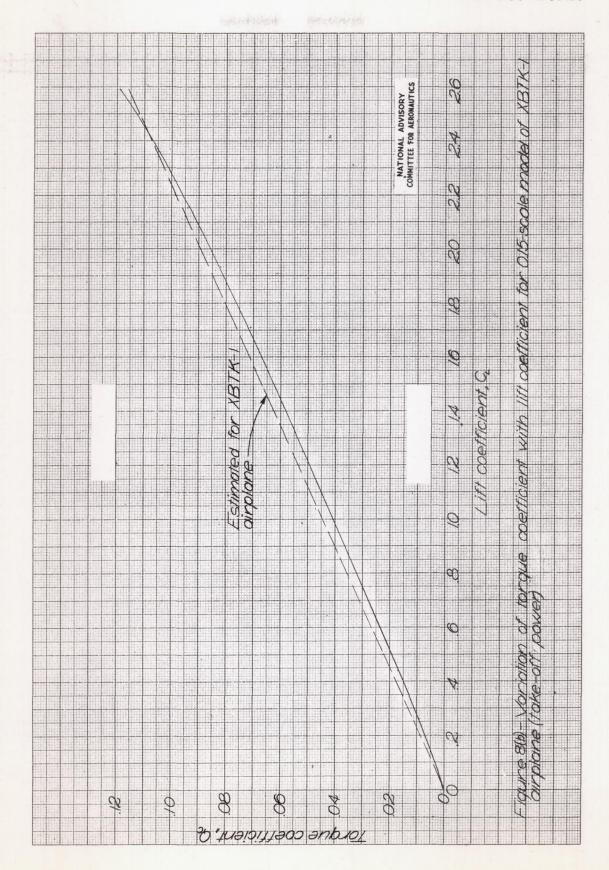


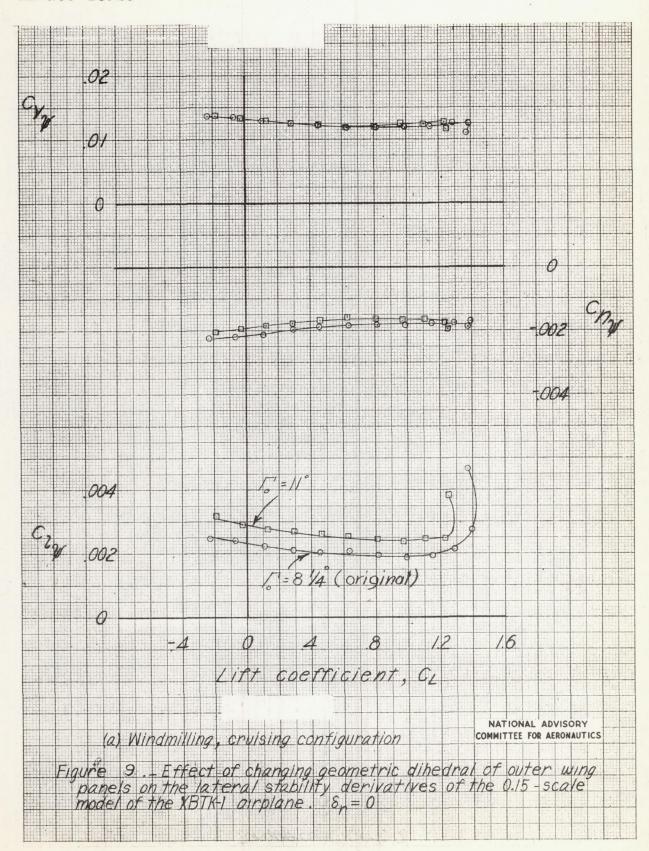
Figure 6 - Drawing of the vertical tail of the 0.15 scale model of the XBTK-I airplane

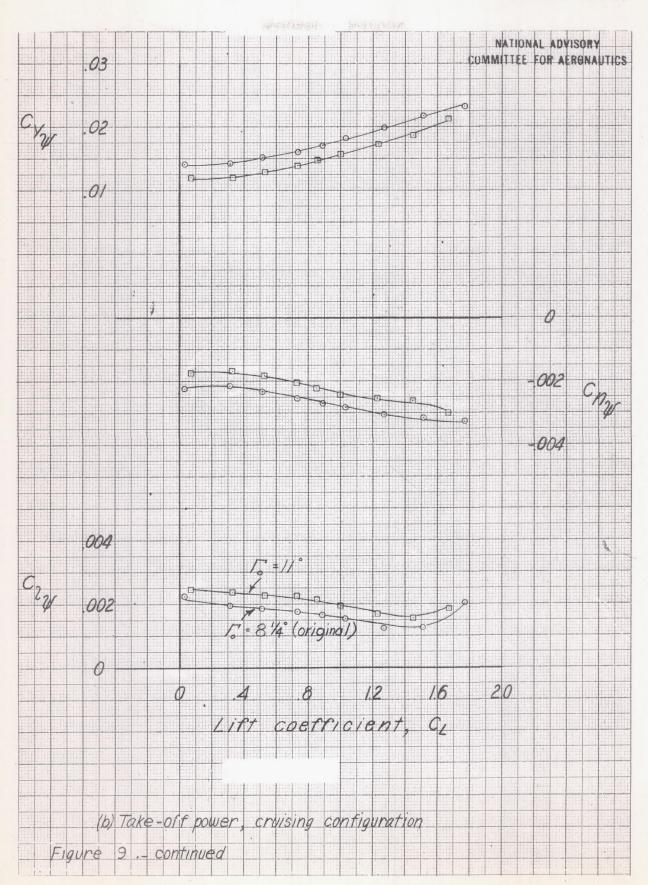
NATIONAL ADVISORY
COMMITTEE FOR AERONAUTICS

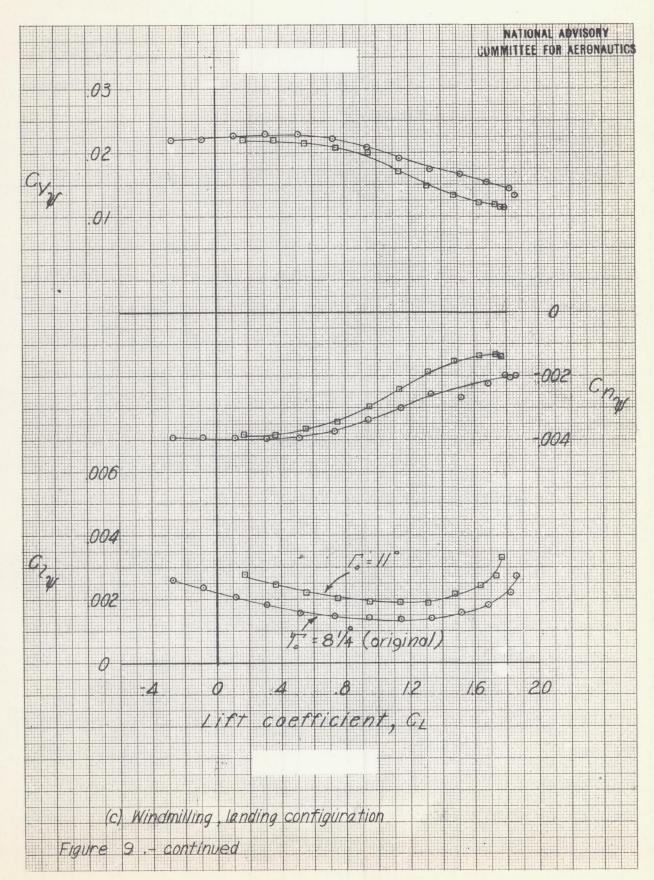


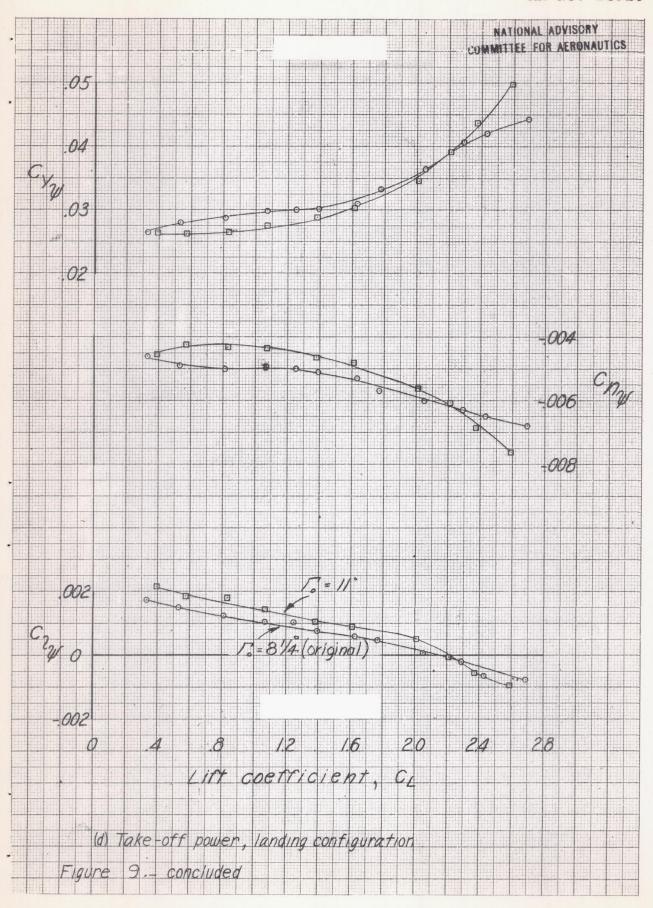


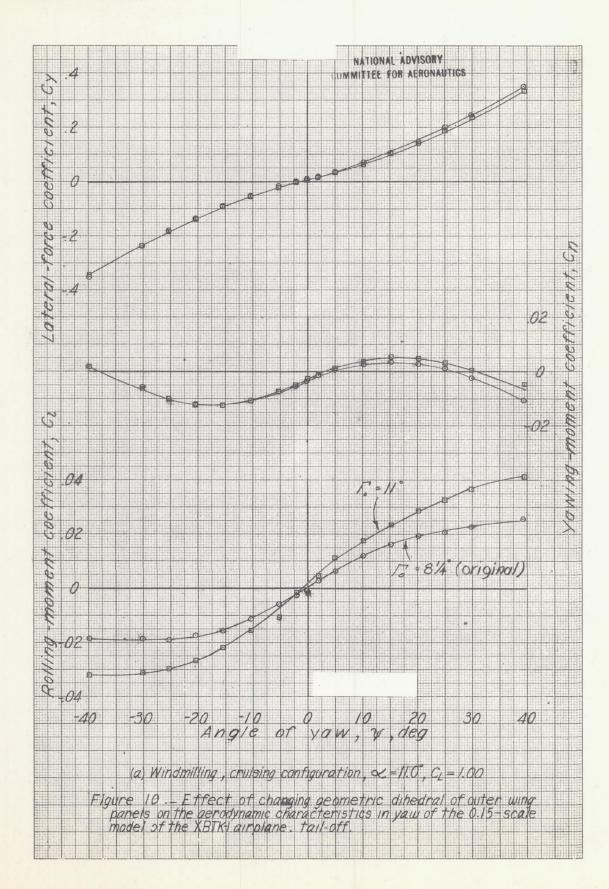


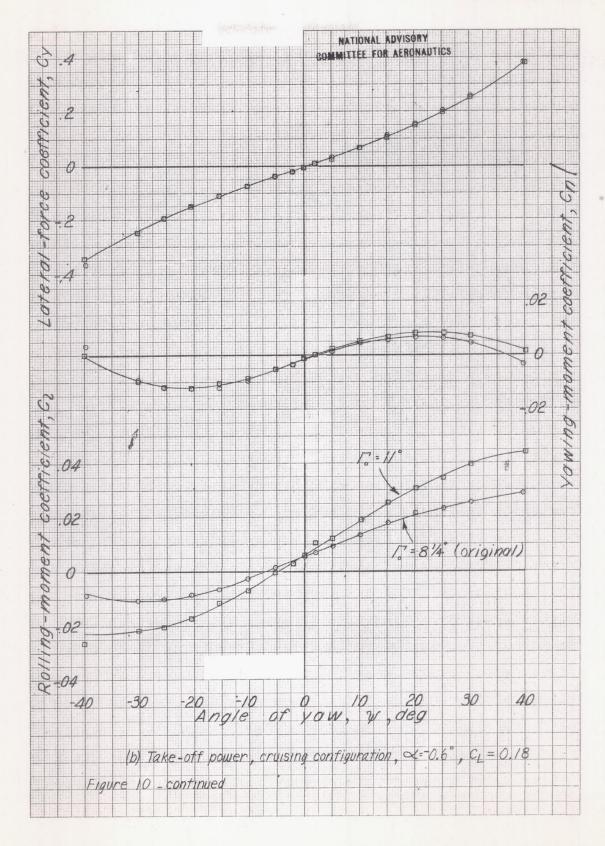


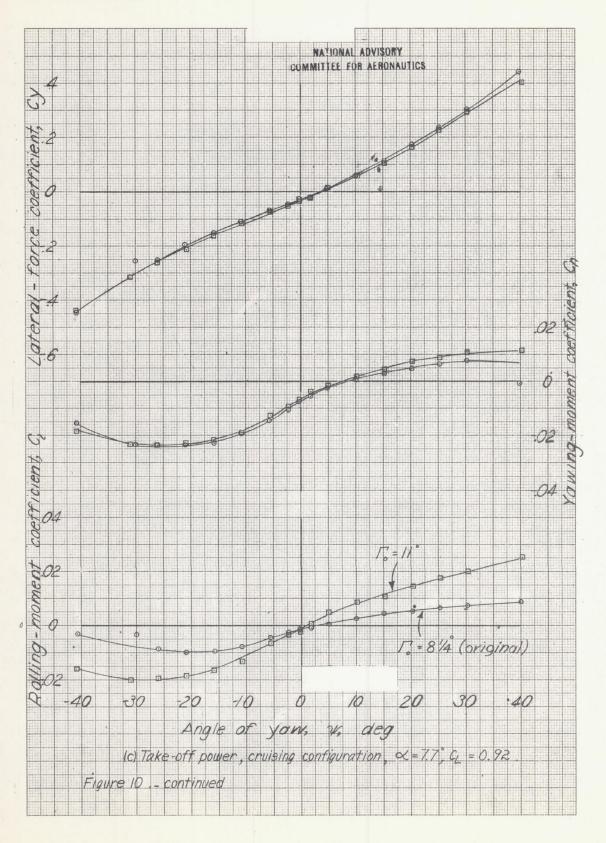


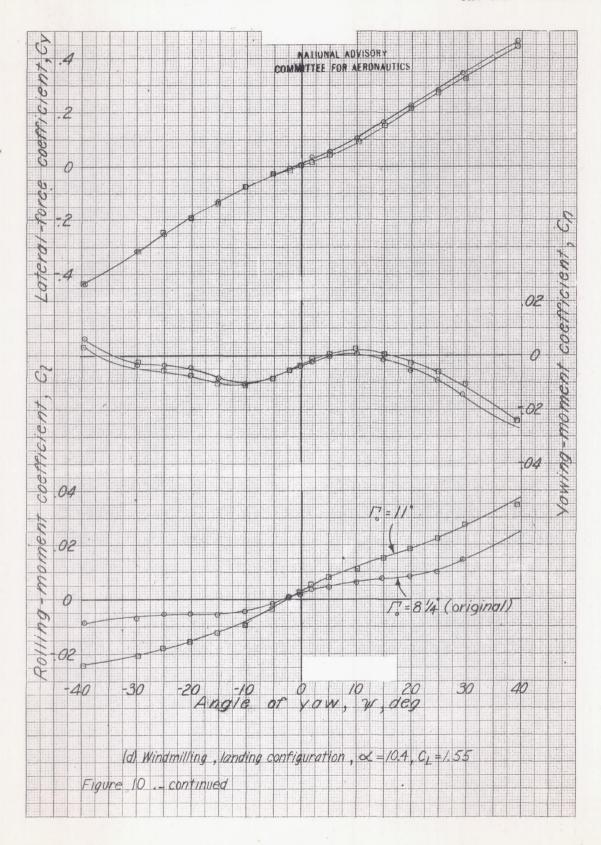


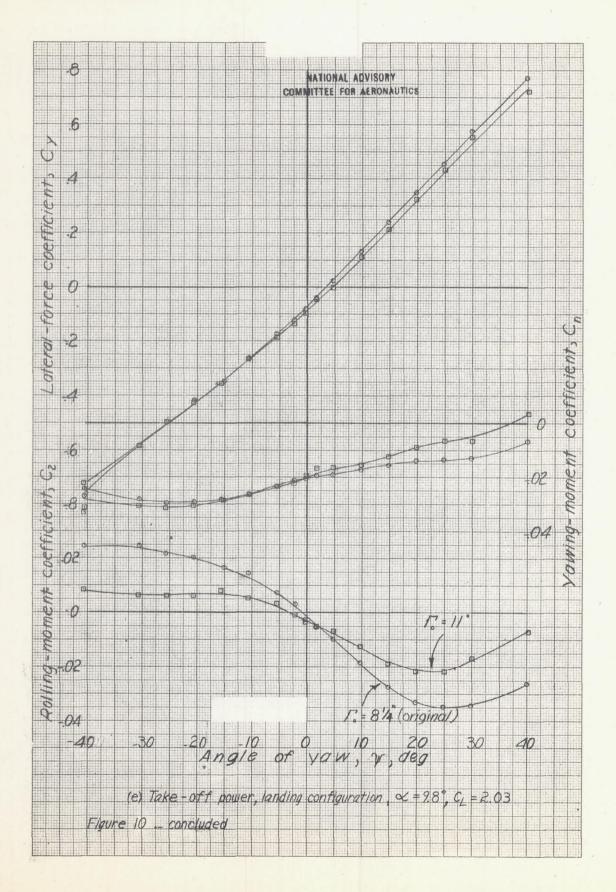


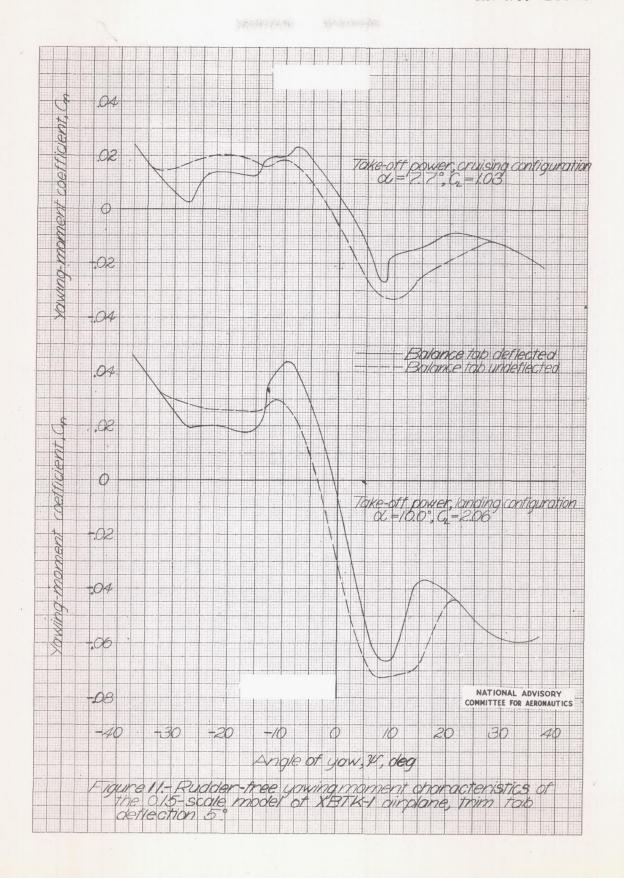


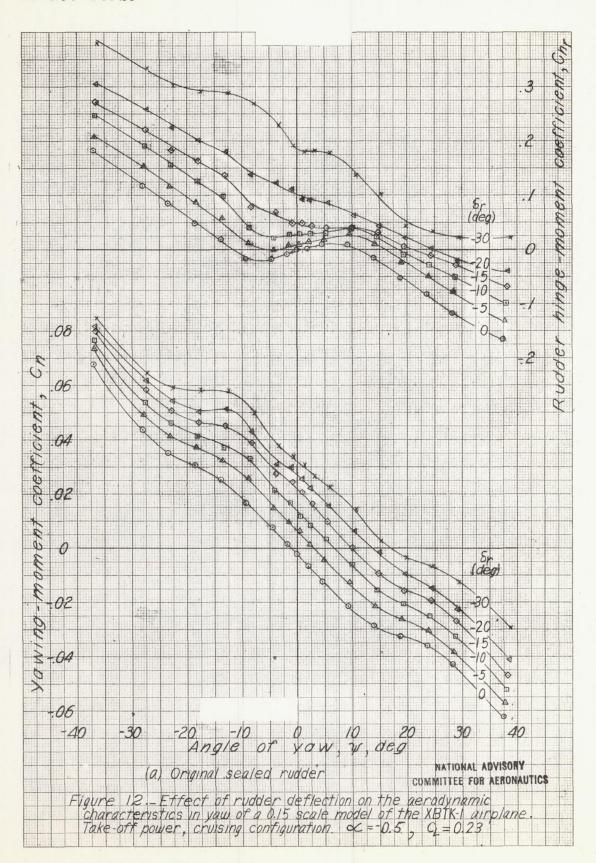


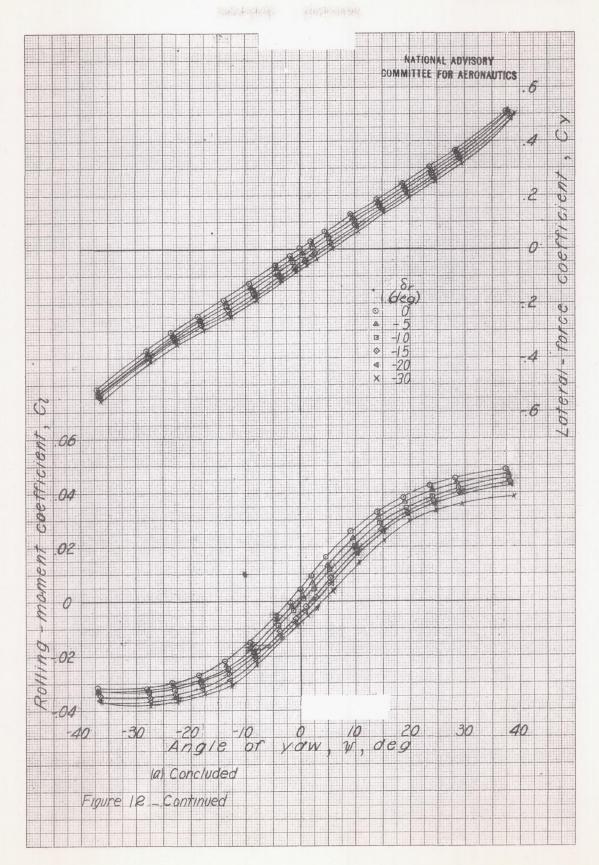


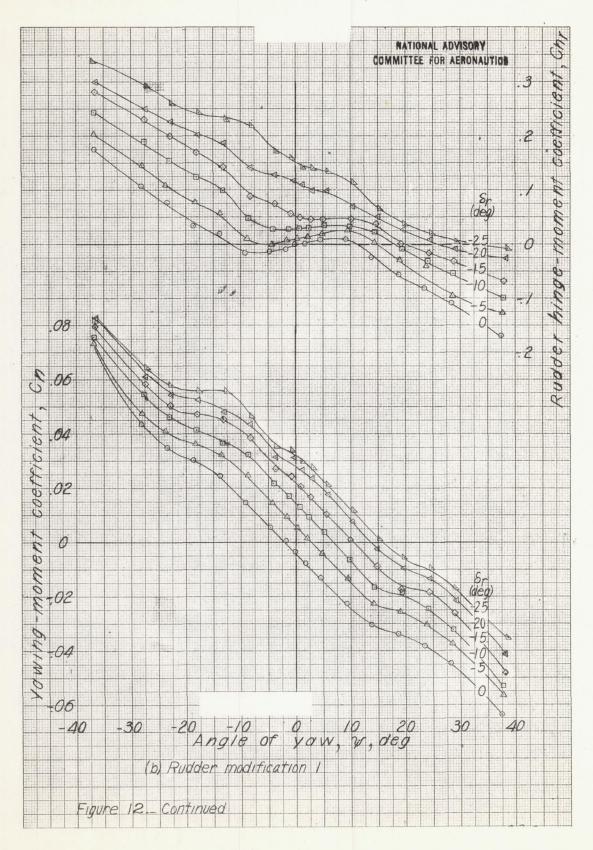


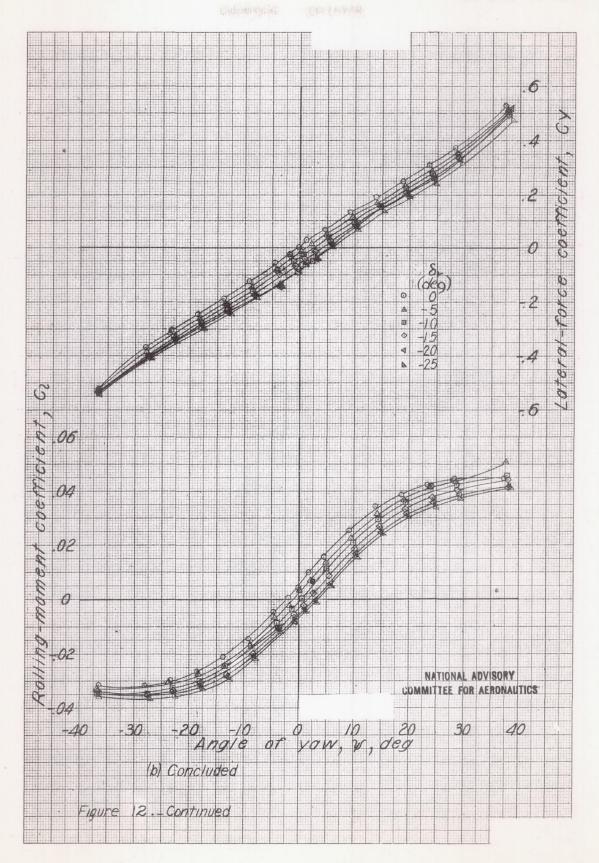


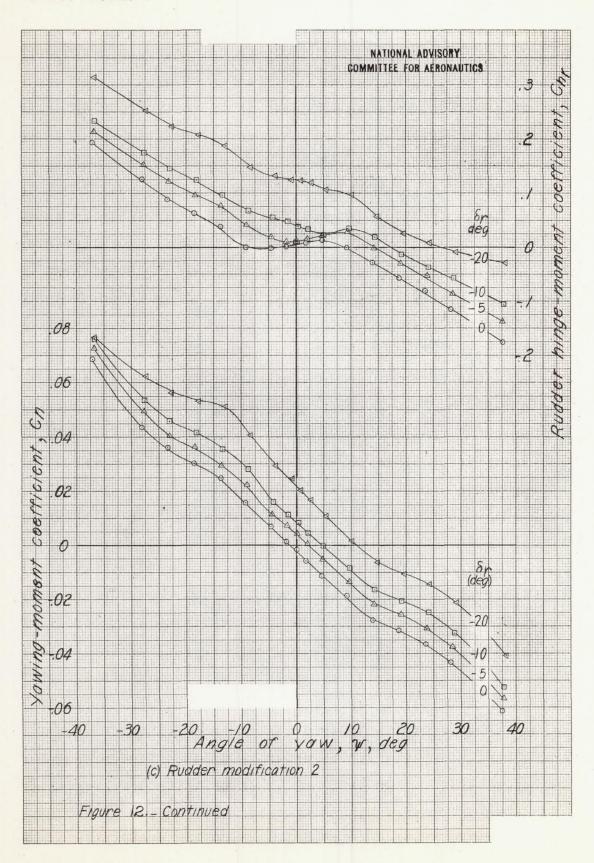


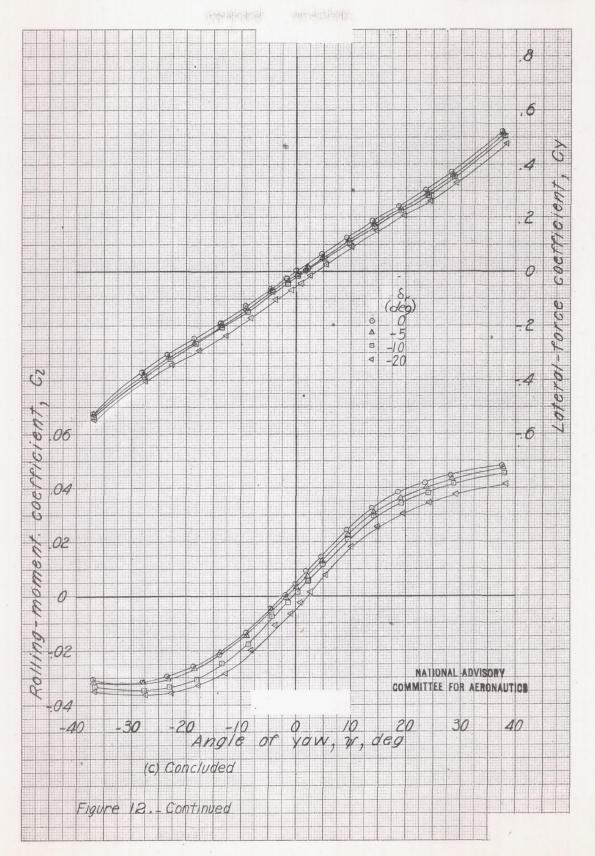


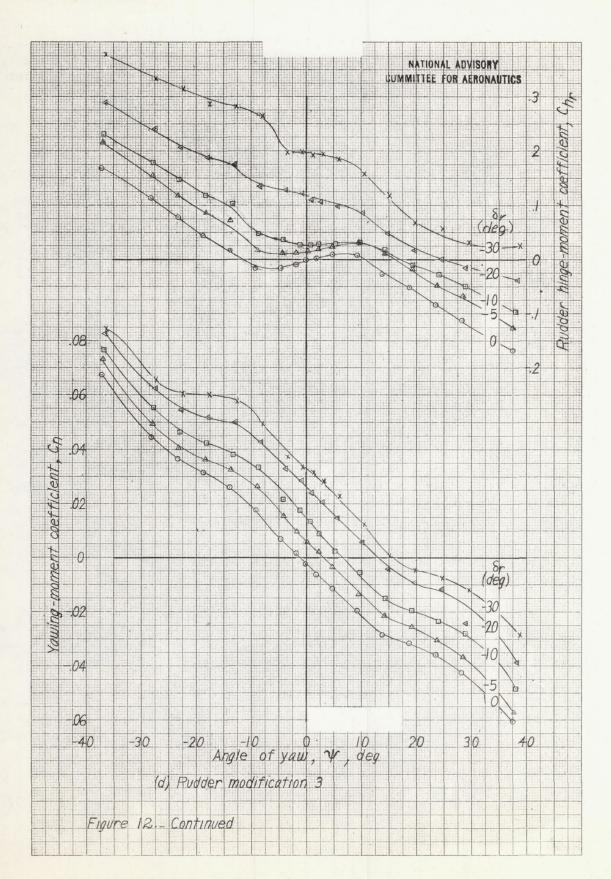


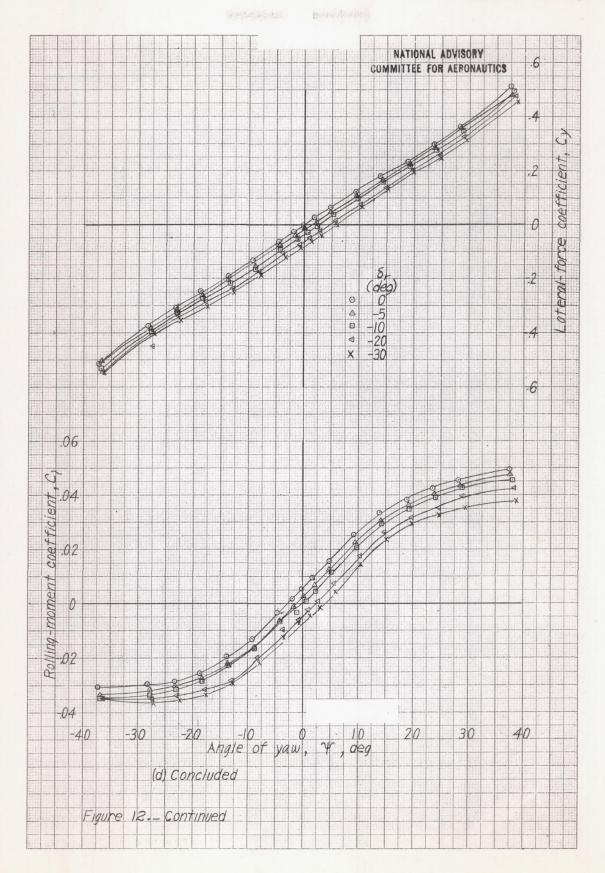


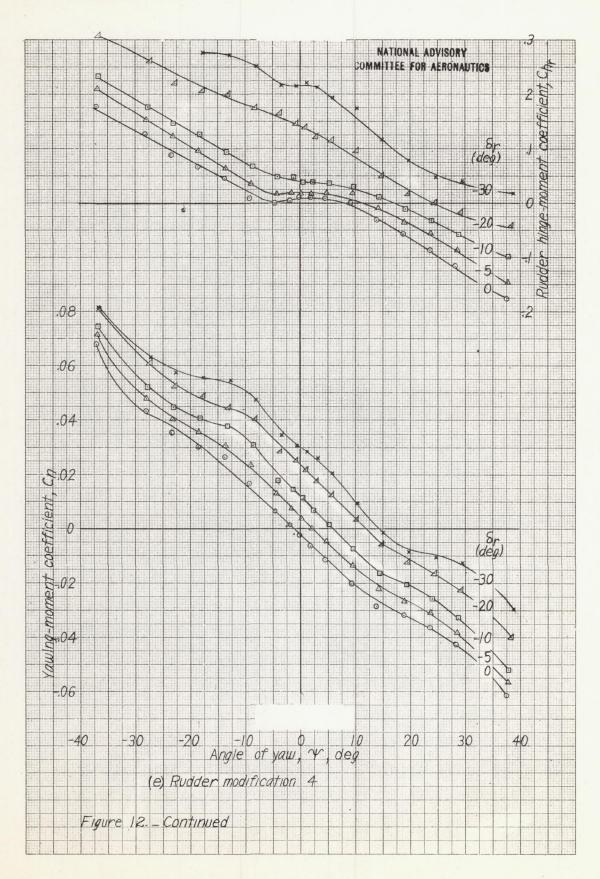


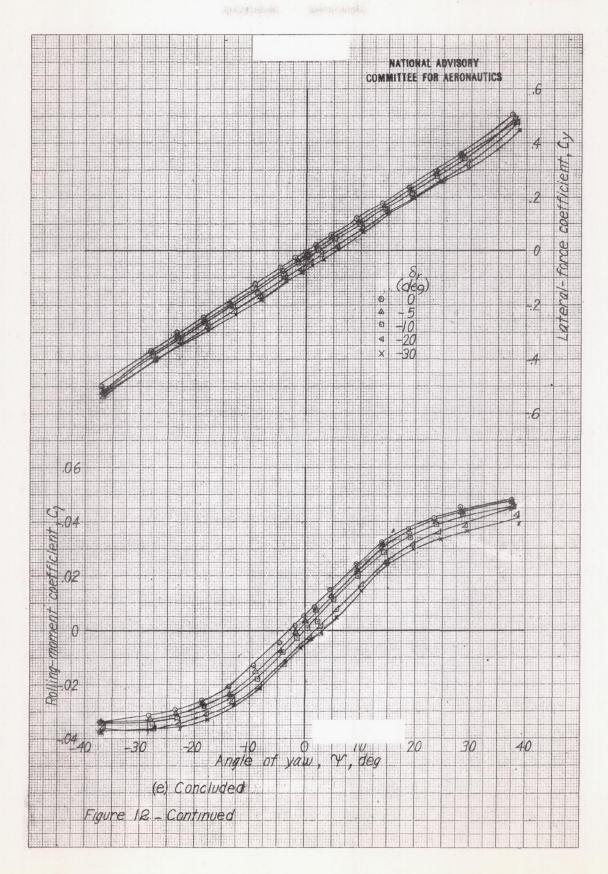


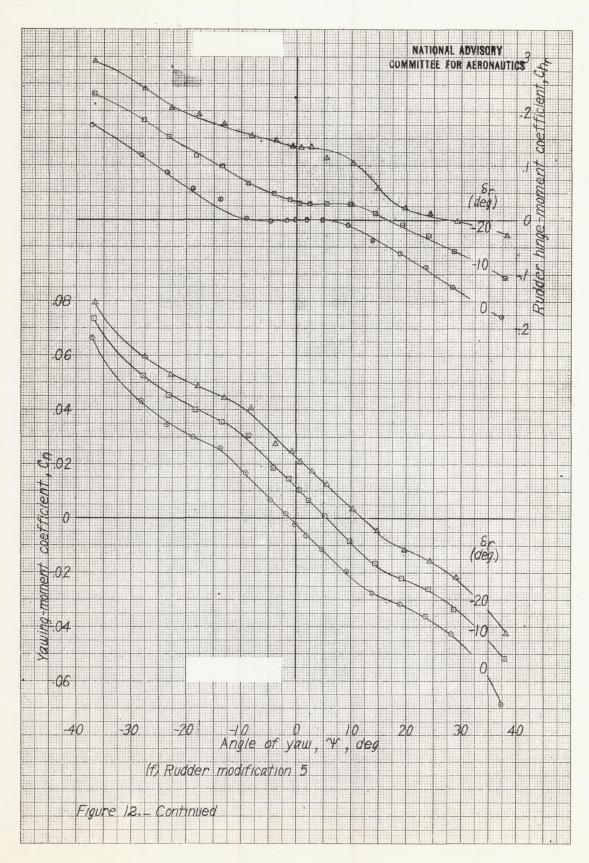


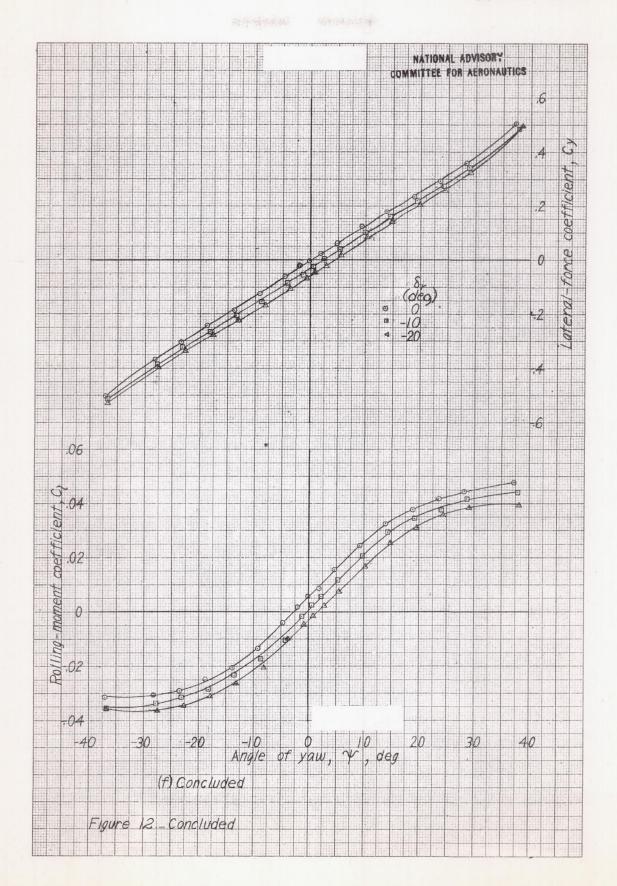


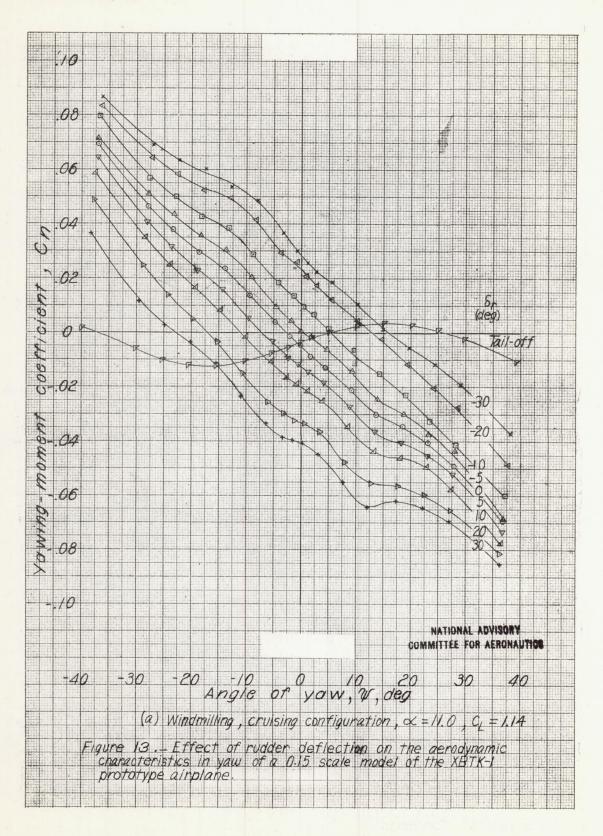


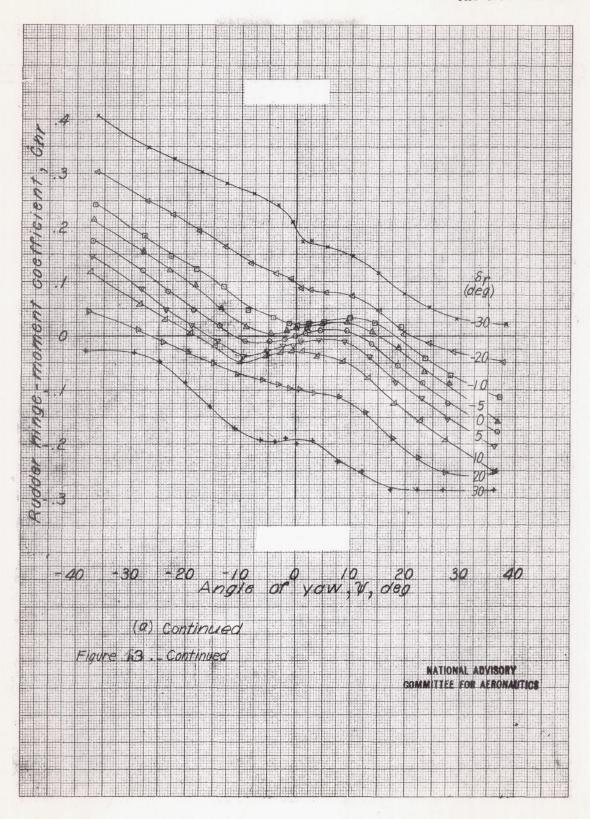


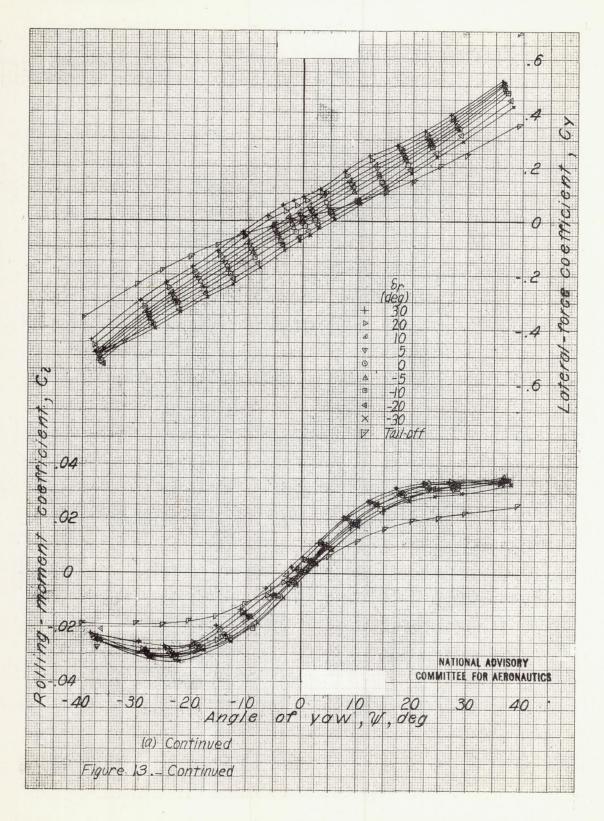


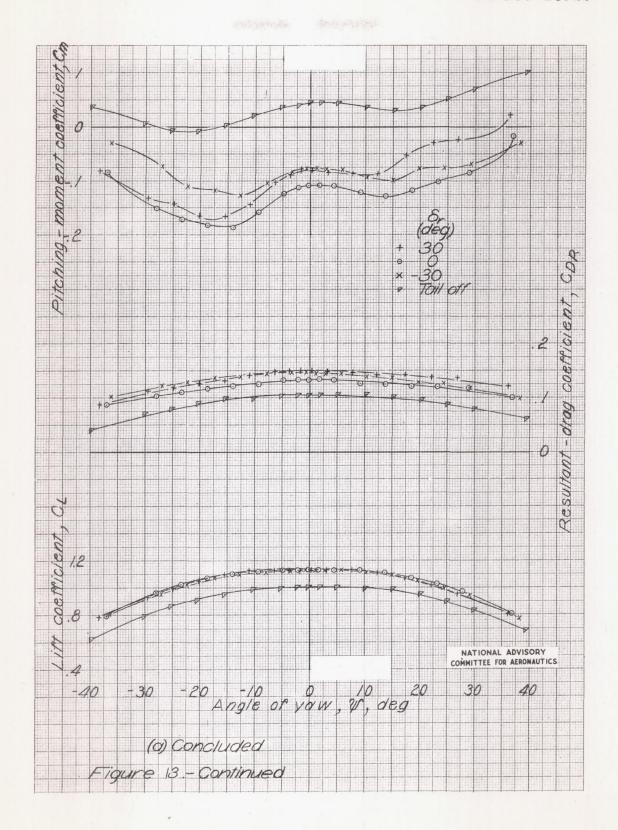


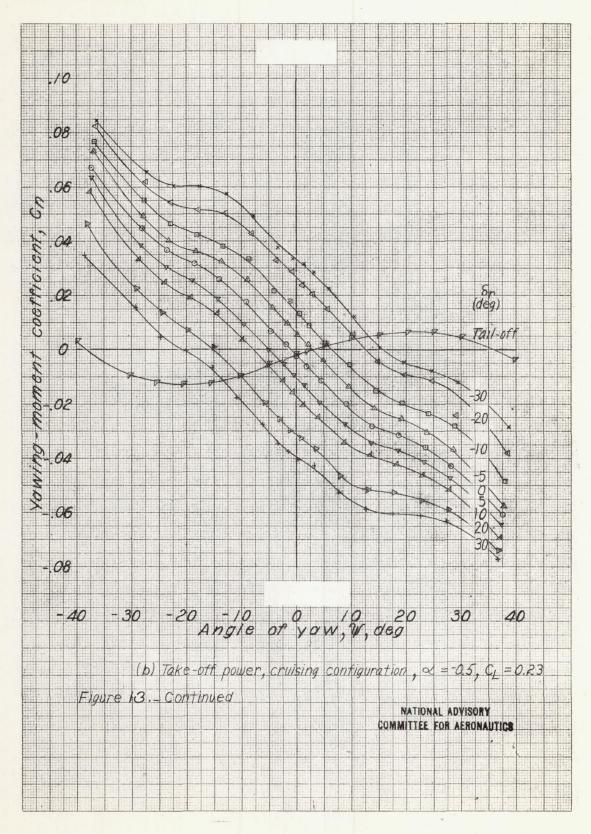


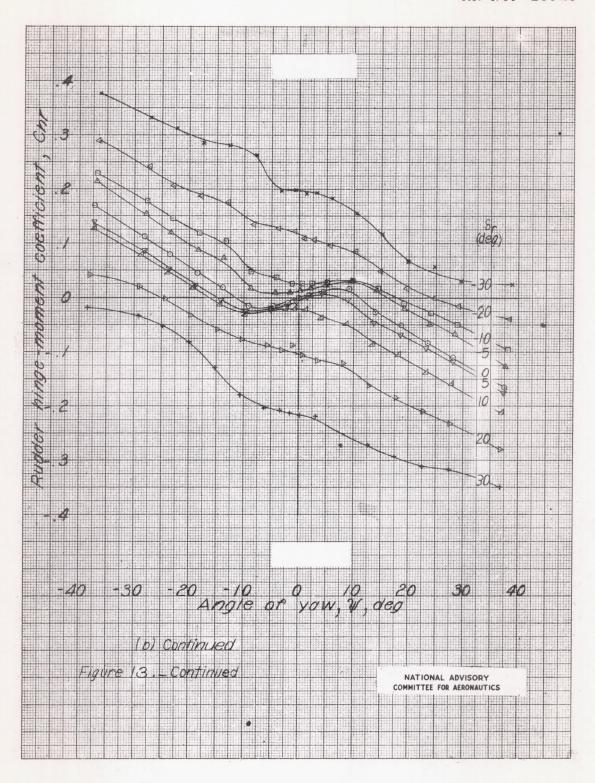




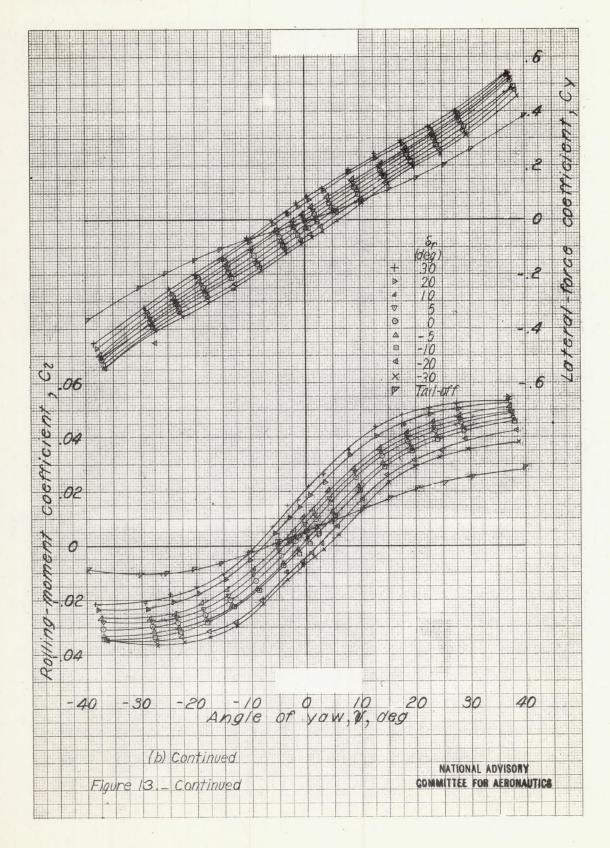


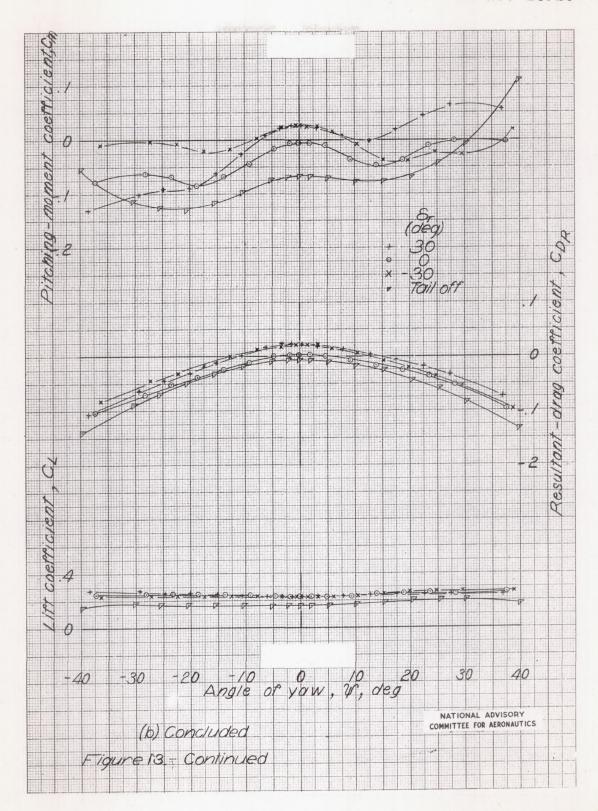


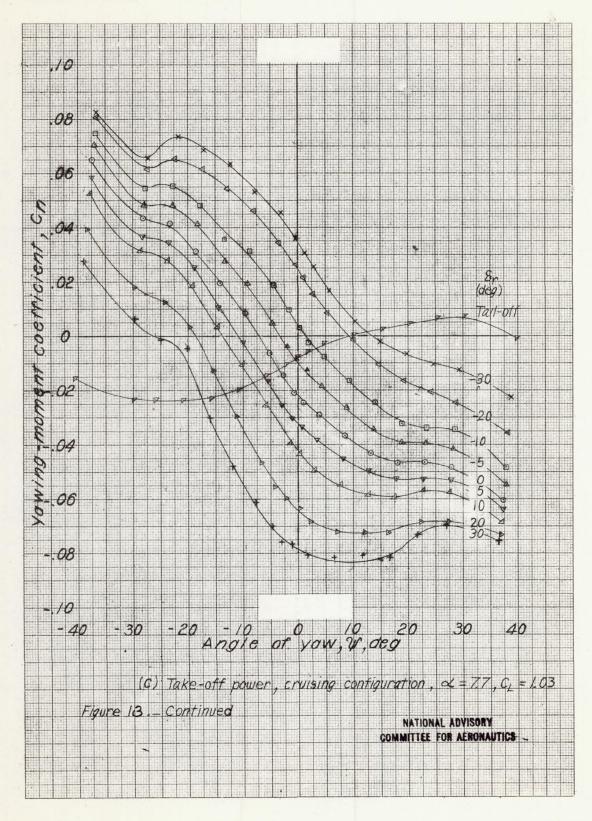


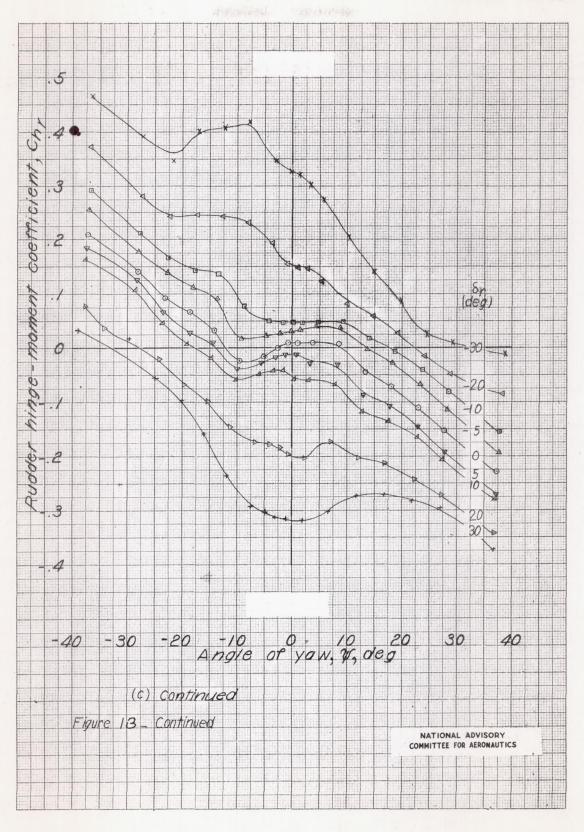


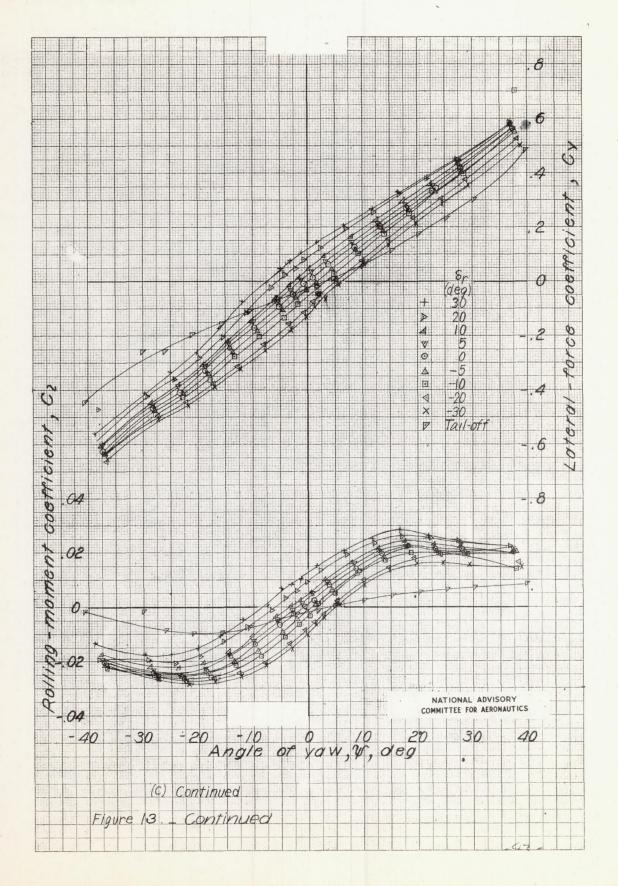
Charles and the state of the st

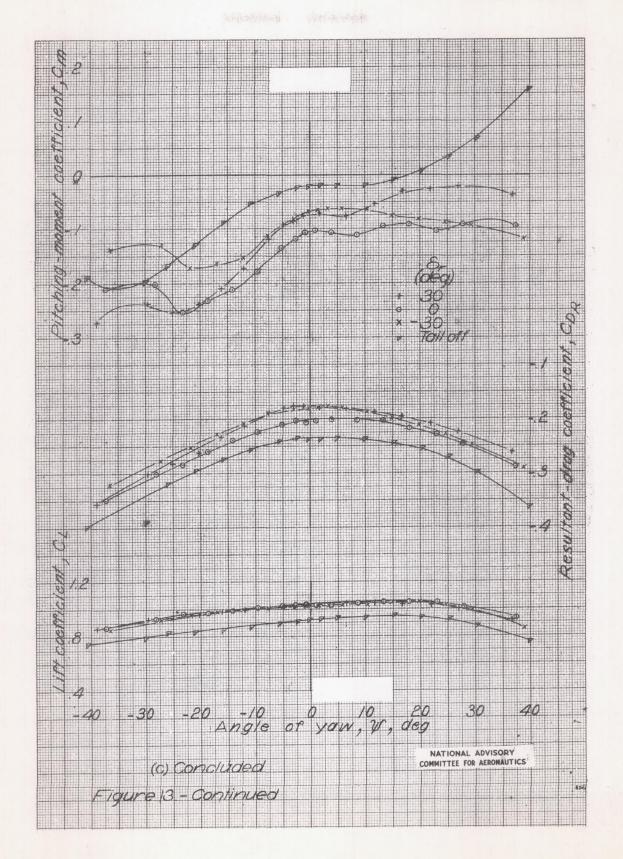


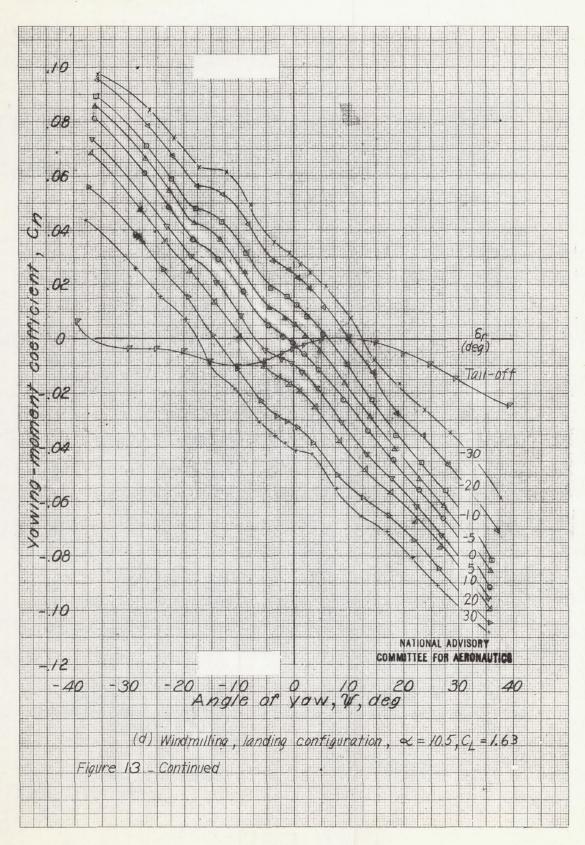


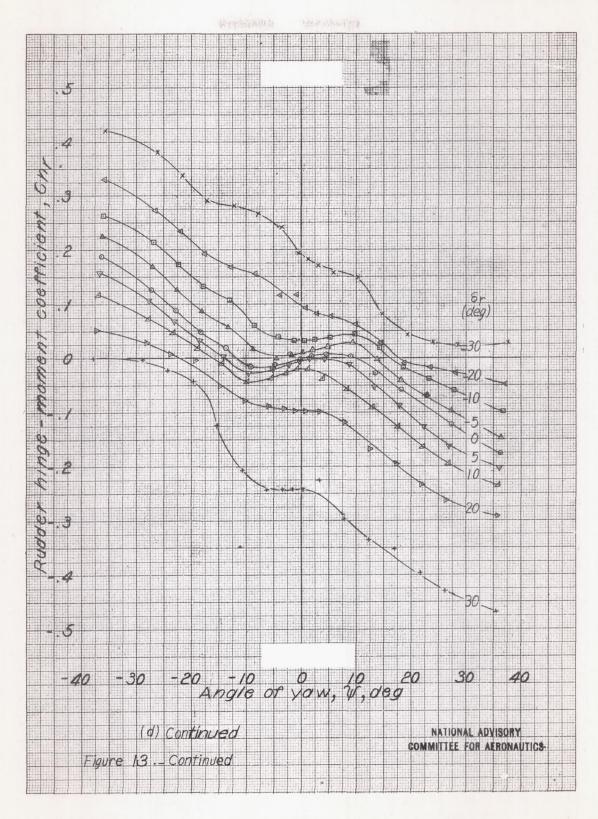


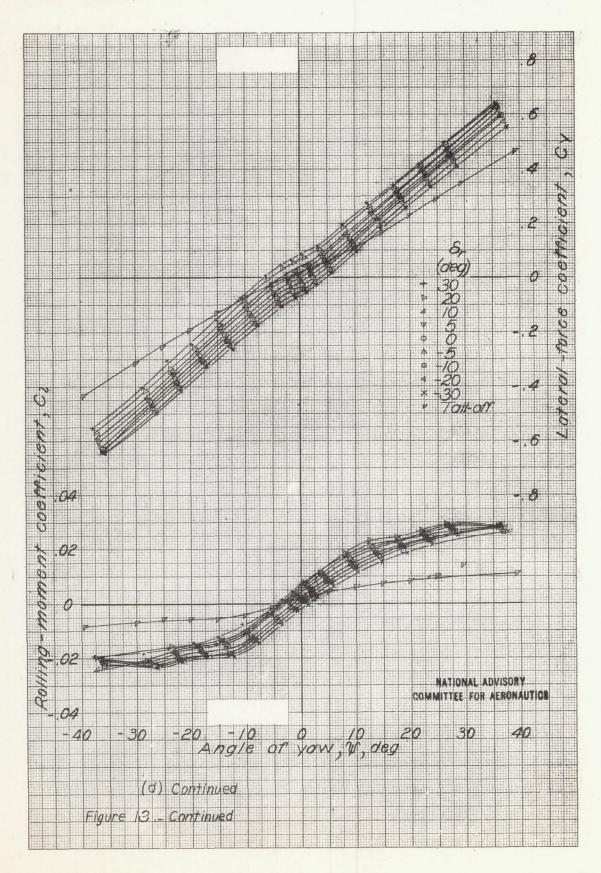


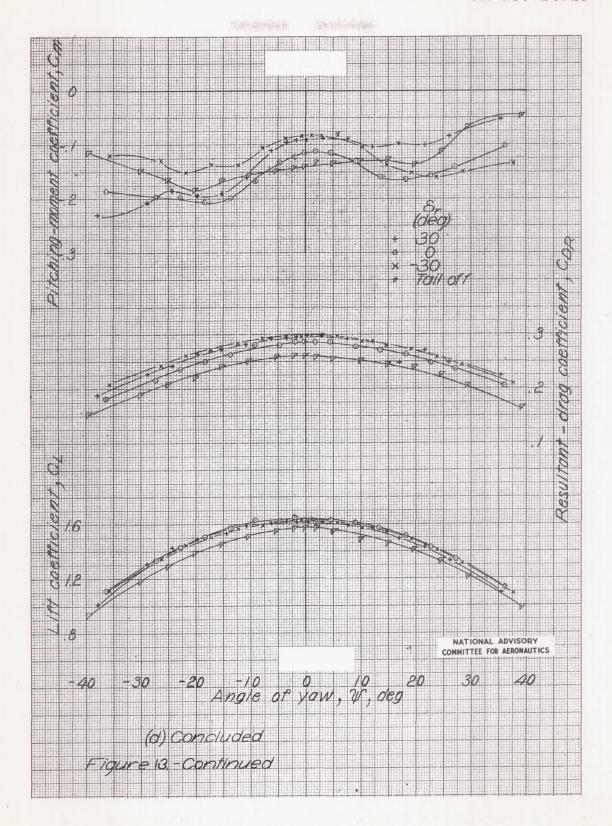


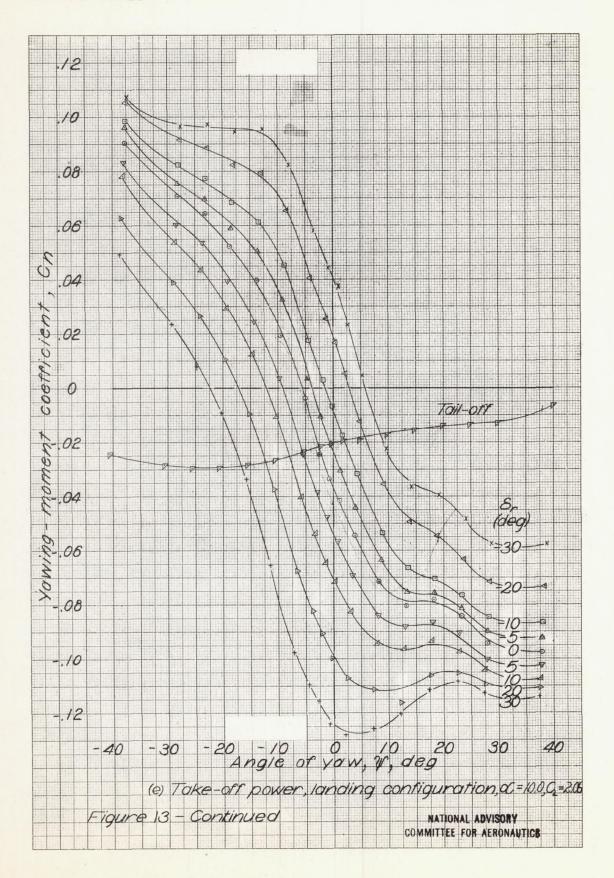


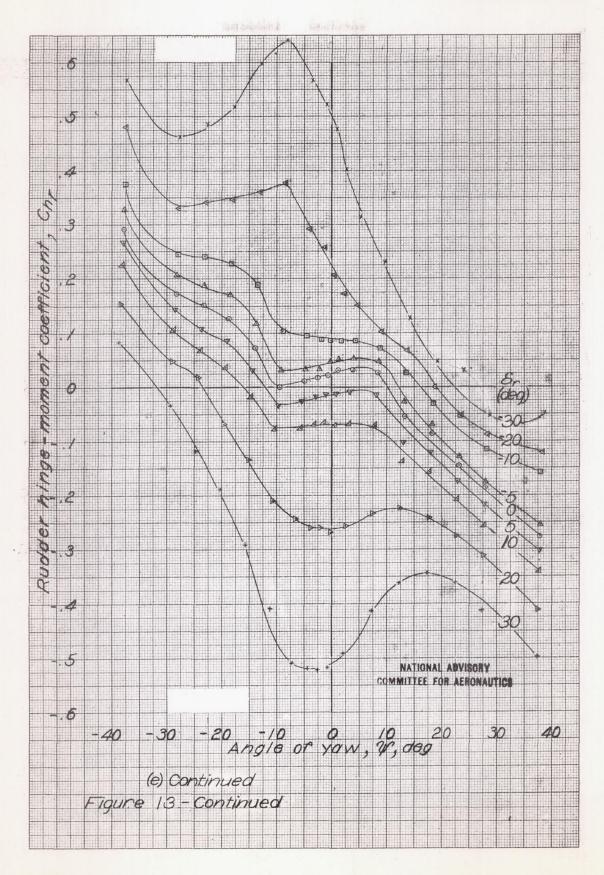




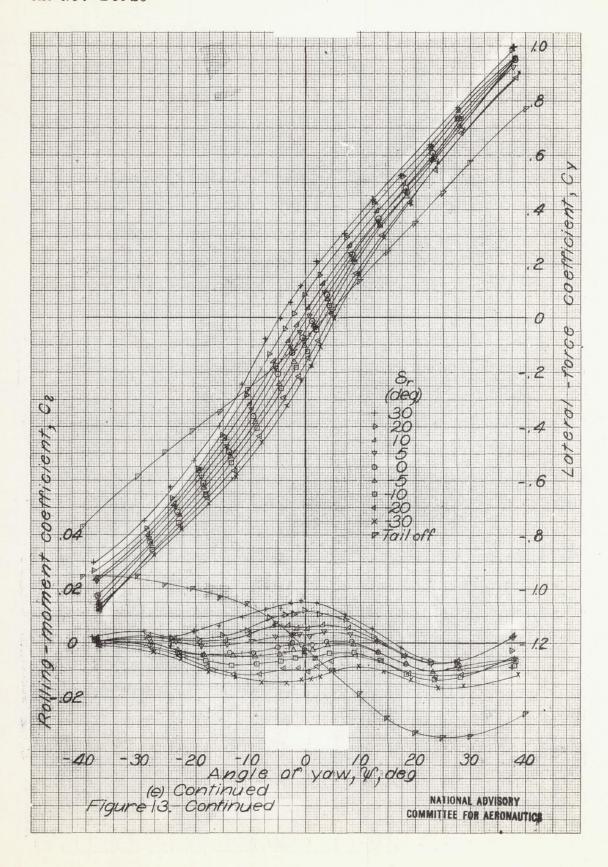


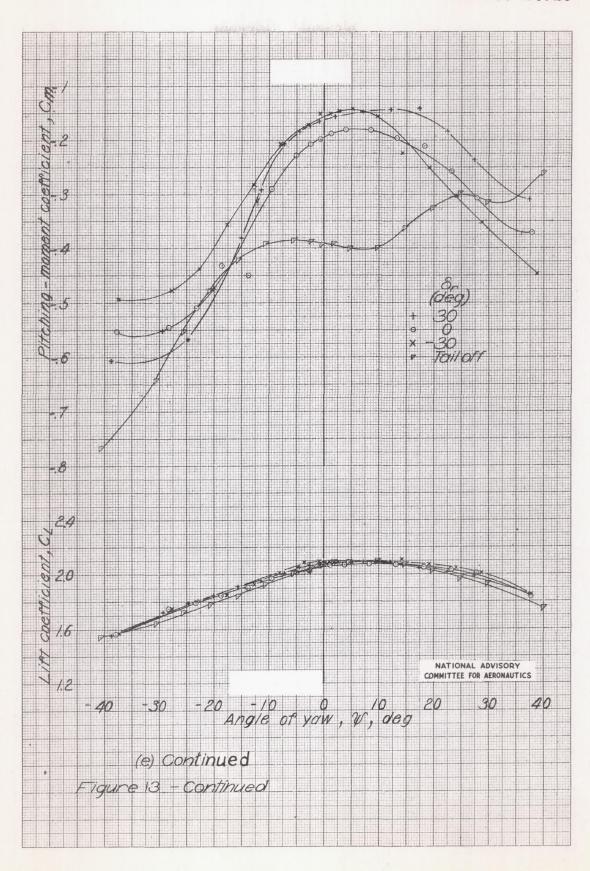




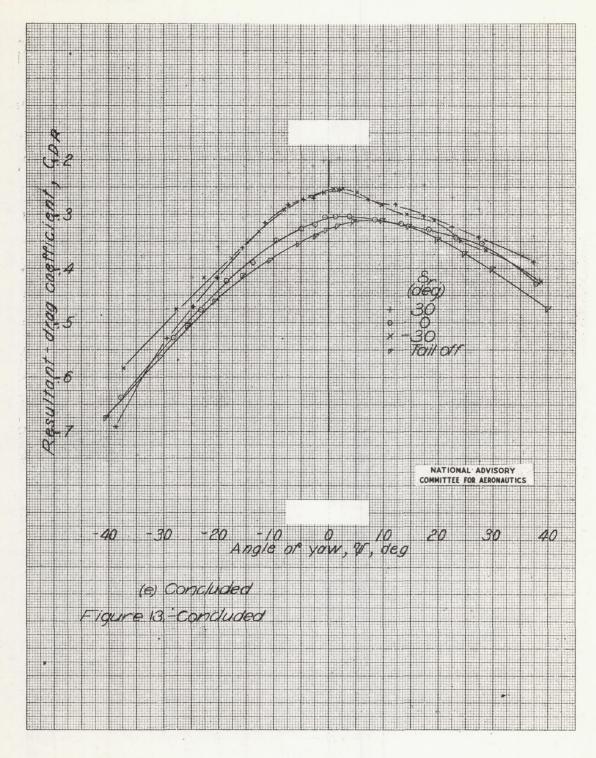


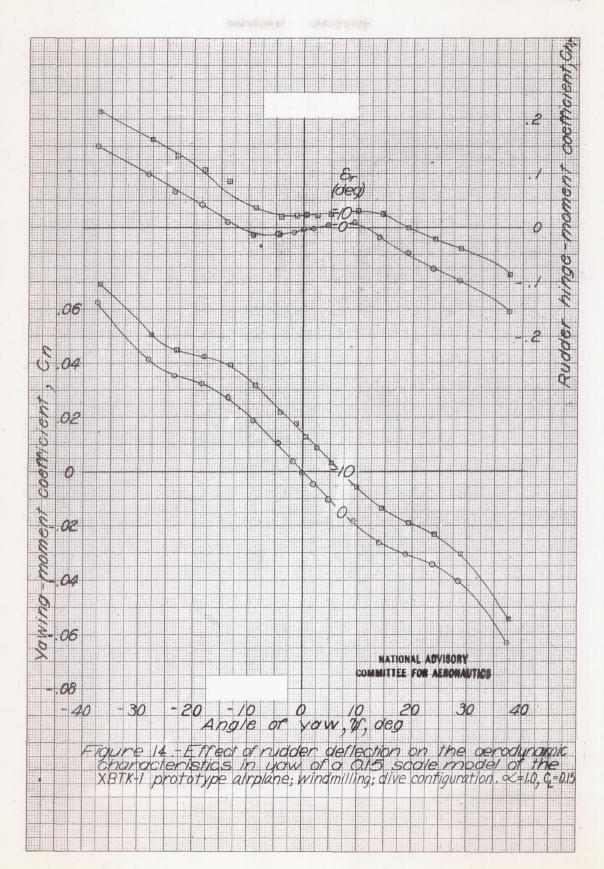
"我也可以对对我们事" "有你的我们的事情



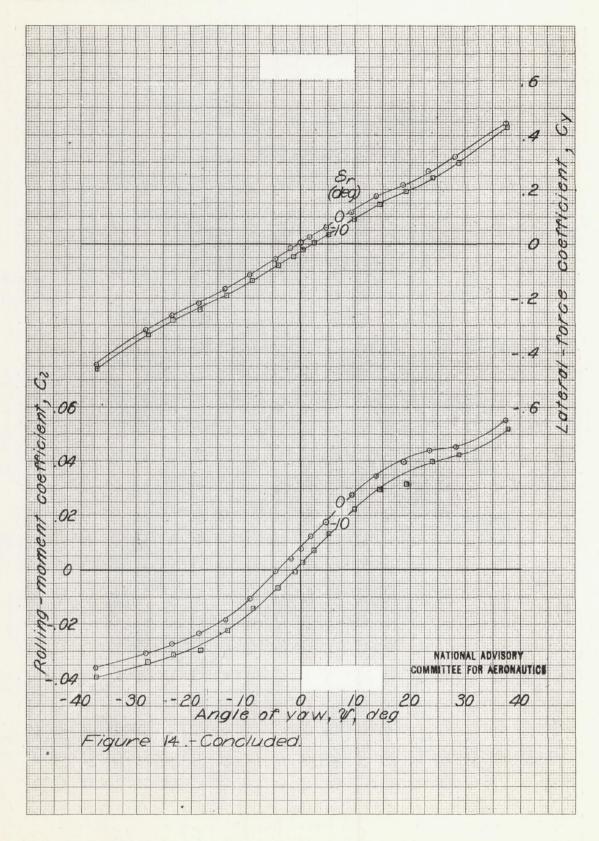


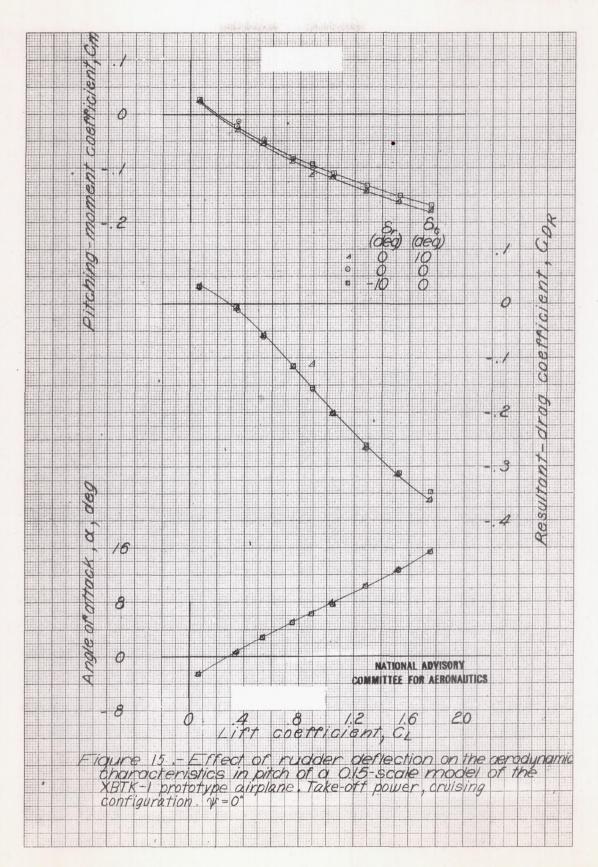
"我们还能够的第三人称形式的原则"。



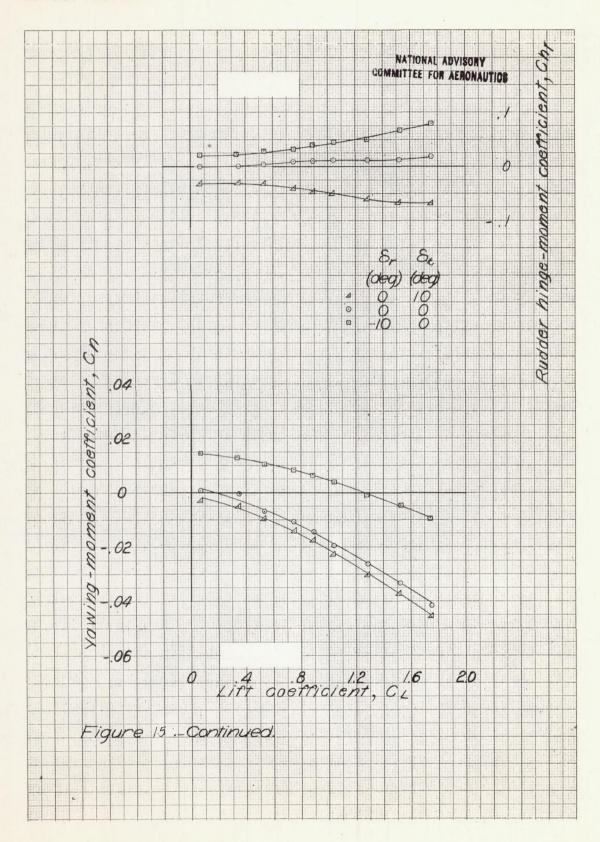


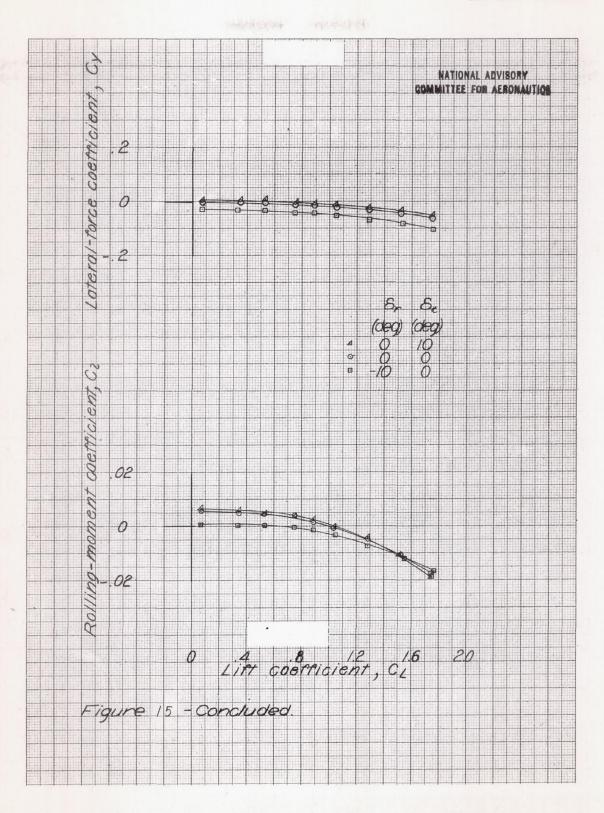
Hippinghophyl Subbillion St.





· 地名第4年的第三人称单数





10年4年2月2日中央 - 10年2月1日中央日本の中国

